A new kannemeyeriiform dicynodont (Synapsida) from a Late Triassic vertebrate assemblage in west Texas, U.S.A.

Bill D. Mueller, Adam K. Huttenlocker, Bryan J. Small, James L. Pinto, Kendra Dean-Wallace & Sankar Chatterjee

View supplementary material

Published online: 03 Nov 2023.

Submit your article to this journal

View related articles

View Crossmark data

Check for updates

ARTICLE

A NEW KANNEMEYERIIFORM DICYNODONT (SYNAPSIDA) FROM A LATE TRIASSIC VERTEBRATE ASSEMBLAGE IN WEST TEXAS, U.S.A.

BILL D. MUELLER,[1]† ADAM K. HUTTENLOCKER, [2]* BRYAN J. SMALL,[1] JAMES L. PINTO,[3]
KENDRA DEAN-WALLACE,[1] and SANKAR CHATTERJEE[1]
[1]Museum of Texas Tech University, Lubbock, TX 79409, U.S.A., bjsmall2008@gmail.com; kendra.dean@ttu.edu;
sankar.chatterjee@ttu.edu;
[2]Department of Integrative Anatomical Sciences, University of Southern California, Los Angeles, CA 90033, U.S.A.,
ahuttenlocker@gmail.com;
[3]Department of Integrative Biology and Museum of Paleontology, University of California, Berkeley, CA 94720-4780, U.S.A.,
jameslpinto@berkeley.edu

ABSTRACT—A new kannemeyeriiform dicynodont is described from the Upper Triassic Tecovas Formation (Dockum Group) of west Texas, U.S.A. The taxon, *Argodicynodon boreni* gen. et sp. nov., is diagnosed by numerous cranial characters including: squamosal-interparietal sutural contact broad and interdigitating; tall, narrow intertemporal region formed by the parietals with long postorbitals forming the lateral face of the dorsal platform; interparietal forms knobby, bilobed exostoses that wedge between the parietals to form a W-shaped outline in dorsal view; basioccipital and exoccipital contributions to the occipital condyle are distinct, and the dorsal fossa separating the exoccipitals is deeply incised and dorsoventrally deep; caniniform process of the maxilla is dorsoventrally deep and well developed; and an elongated tab-like medial process of the articular exceeds the width of the quadrate roller. A phylogenetic analysis based on 23 continuous and 176 discrete (numeric) morphological characters and 120 taxa finds *Argodicynodon* conservatively to be a placeriine near the *Placerias* + *Moghreberia* group, representing the oldest placeriine in the southwestern U.S.A. and the first named dicynodont genus from the Dockum Group of Texas. A review of Euramerican dicynodont records exposes their hidden diversity and abundance in Laurasia during the Late Triassic. The records of *Argodicynodon* and other previously undescribed dicynodont fossils from nearby localities underscores the diversity of non-*Placerias* dicynodonts in the North American Upper Triassic.

http://zoobank.org/urn:lsid:zoobank.org:pub:AB9B7ABC-6C84-4B04-909F-F1DA114030AB

INTRODUCTION

Dicynodonts are among the best-known and most diverse terrestrial vertebrate herbivores from Middle Permian through Upper Triassic rocks. Given their richness and local abundances, they have been widely utilized for global biostratigraphic correlation (Angielczyk, 2001; Angielczyk & Kurkin, 2003; Angielczyk et al., 2014a, 2014b; Battail, 1993; Groenewald & Kitching, 1995; King, 1993; Kitching, 1995a, 1995b; Lucas, 1995; Rubidge et al., 1995; Rubidge, 2005; Smith & Keyser, 1995a, 1995b, 1995c, 1995d; Smith et al., 2020). Although one clade of dicynodonts achieved a near cosmopolitan distribution by the Late Triassic —the Kannemeyeriiformes—their predominance was eventually supplanted by other contemporary herbivore clades (including

archosauromorphs) and the group ultimately became extinct in Gondwanan basins by the end of the Norian stage (Kammerer & Ordoñez, 2021; Sookias et al., 2012). In the Upper Triassic of Laurasia, dicynodont fossils are still more elusive, with only a handful of kannemeyeriiforms known from North America and central Europe (Dzik et al., 2008; Schoch, 2012; Sulej et al., 2011; Sulej & Niedźwiedzki, 2019; Szczygielski & Sulej, 2021). The sparse North American Triassic record of dicynodonts implies a lack of diversity and importance in Late Triassic communities, but could be biased by a generally poor Carnian and early Norian fossil record in the northern hemisphere.

Review of North American Dicynodonts

Dicynodont occurrences in the Triassic of North America, while scarce, are noteworthy for documenting some degree of continental diversity and interbasinal endemism following the Triassic Laurasian pattern (Table 1). The oldest North American dicynodonts are represented by fragmentary, indeterminate elements, and tracks from the Middle Triassic Holbrook

---

TABLE 1. List of published North American Triassic dicynodonts.

Taxon	Formation/Age	Reference
Dicynodontia indet.	Moenkopi/Anisian	Nesbitt & Angielczyk (2002)
Kannemeyeriiformes indet.	Wolfville, Economy Member/ Anisian-Ladinian	Sues et al. (2022)
Placerias hesternus	Chinle/Norian	Lucas (1904)
Placerias gigas	Chinle/Norian	Camp & Welles (1956)
Eubrachiosaurus browni	Popo Agie/Norian	Williston (1904)
Stahleckeriidae indet.	Santa Rosa/Norian	Lucas & Hunt (1993a); Kammerer et al. (2013)
Dicynodontia indet. (Numerous localities)	Tecovas/Norian	Mueller (2016); this study
Argodicynodon boreni	Tecovas/Norian	Mueller (2016); this study
Placerias hesternus	Pekin/Carnian	Baird & Patterson (1968); Kammerer et al. (2013)
Stahleckeriidae indet.	Pekin/Carnian	Green et al. (2005); Kammerer et al. (2013)
Kannemeyeriiformes indet.	Wolfville, Evangeline Member/Carnian	Sues & Olsen (2015)

Member of the Moenkopi Formation (Anisian) in the southwestern U.S.A. (Hunt et al., 1993; Nesbitt & Angielczyk, 2002), as well as fragmentary remains from the Middle Triassic (Anisian–Ladinian) section of the Economy Member of the Wolfville Formation (Newark Supergroup), Fundy Basin, Nova Scotia, Canada (Baird & Olsen, 1983; Sues & Olsen, 2015). The first valid description of a dicynodont in the North American Triassic was published in 1904 when Lucas erected *Placerias hesternus* based on a humerus (USNM 2198) collected by Barnum Brown from the Blue Mesa Member of the Petrified Forest Member of the Chinle Formation (Norian) near Tanner's Crossing, Arizona. Since then, discoveries of North American Triassic dicynodonts have been uncommon and, except for the stahleckeriid *Placerias hesternus* (= *P. gigas*; Lucas & Hunt, 1993a), other records are poorly represented by isolated or incomplete remains (Camp & Welles, 1956; Kammerer et al., 2013).

Williston (1904) erected two dicynodont taxa, *Eubrachiosaurus browni* and *Brachybrachium brevipes*, for specimens collected from the Popo Agie Formation (Norian) in Fremont County, Wyoming. *Eubrachiosaurus browni* was erected for an incomplete, crushed humerus (FMNH UC 633), with a referred scapula, ischium, and pubis. *Brachybrachium brevipes* was also erected for an incomplete left humerus. Globally, most dicynodont species have been described based primarily on cranial material, making systematic determinations difficult for these fragmentary taxa. Camp and Welles (1956) considered *Eubrachiosaurus* to be a valid taxon. King (1988) retained both of these taxa as valid, but pointed out that the holotype of *B. brevipes* was missing and that it was possibly a junior synonym of *P. hesternus*. *Eubrachiosaurus browni* was considered a synonym of *Placerias hesternus* by Lucas et al. (1993a); however, Long and Murry (1995) considered it was not conspecific and possibly not congeneric to *P. hesternus*. They considered the humerus to be more closely referable to the genus *Ischigualastia*. Kammerer et al. (2013) corroborated the opinion that *Eubrachiosaurus* is a valid stahleckeriid taxon distinct from *Placerias*, firmly establishing at least two separate, nominal stahleckeriid taxa in the Upper Triassic of North America.

Camp and Welles (1956) erected the taxon *Placerias gigas* for the large population of material they described from a quarry

southwest of St. Johns, Arizona. The *Placerias* Quarry has produced parts of some 40 + individuals from the upper Blue Mesa Member of the Chinle Formation (Norian) (Parker & Martz, 2011) with the UCMP collection containing over 1,700 cataloged elements. Lucas and Hunt (1993a), Long and Murry (1995), and Lucas (1998b) considered *P. hesternus* and *P. gigas* to be conspecific as their separation was based only on slight proportional differences in the humerus. Ramezani et al. (2014) determined the age of the *Placerias* Quarry to be approximately 219 Ma or mid-Norian and equivalent to the lower Sonsela Member. That is considerably younger than previously thought (Long and Murry, 1995).

Elsewhere in the southwestern U.S.A, Lucas and Hunt (1993a) documented dicynodont material from the Santa Rosa Formation (lower Norian) in New Mexico, referring it to cf. *Ischigualastia*. The material was a femur (NMMNH P-13001), radius (NMMNH P-13002), scapula (NMMNH P-13003), phalanx (NMMNH P-13004), and axis vertebra (NMMNH P-13005). Long and Murry (1995) concurred that the femur (NMMNH P-13001) did not belong to *Placerias*; however, they disagreed with its referral to cf. *Ischigualastia*. The published description and illustration of the femur indicate that it does not belong to *Placerias* or *Ischigualastia* (Cox, 1965) but does resemble the femur of *Stahleckeria*, and the associated NMMNH material would indicate that it was not diagnostic below the family level (Kammerer et al., 2013).

In eastern North America, *Placerias* specimens (Baird & Patterson, 1968; Huber et al., 1993) and a presumed non-*Placerias* kannemeyeriiform (Green et al., 2005) are known from the Carnian-aged Pekin Formation (Newark Supergroup) of North Carolina. *Placerias* was provisionally reported from the Upper Triassic Pekin Formation (Newark Supergroup) of North Carolina by Baird and Patterson (1968). This material, although mostly fragmentary, is sufficiently well preserved that it is diagnostic to *Placerias hesternus* (Lucas, 1998b; B.D.M. pers. obs.). Non-*Placerias* kannemeyeriiform dicynodont material from the Pekin Formation of North Carolina has also been reported by Green et al. (2005), but has yet to be described in detail; a posterior jaw fragment and the posterior portion of the skeleton (Green, 2012:fig. 7.1) were diagnostic enough to determine they were a non-*Placerias* stahleckeriid (Kammerer et al., 2013). In addition, fragmentary kannemeyeriiform remains contemporary with the cynodont *Arctotraversodon* (Hopson, 1984; Sues et al., 1992) have been long reported in the Upper Triassic (Carnian) Evangeline Member of the Wolfville Formation, Nova Scotia (Baird & Olsen, 1983; Sues & Olsen, 2015). All of the named North American dicynodonts belong to the Stahleckeriidae (Cox, 1965), the only clade understood to have dispersed across Eurasia by late Carnian to Norian times (Camp & Welles, 1956; Sulej & Niedźwiedzki, 2019; Szczygielski & Sulej, 2021).

Present Study

Only recently have dicynodonts been reported from the Dockum Group of Texas, including specimens from the Boren Quarry (MOTT VPL 3869; Fig. 1), but none has been described in detail (Lehman & Chatterjee, 2005; Martz, 2008; Martz et al., 2013; Mueller & Chatterjee, 2007). The Museum of Texas Tech now houses over 36 dicynodont elements from eight localities in the Dockum Group (Tables 2, 3). Numerous elements of a new dicynodont recovered from the Boren Quarry (Mueller & Chatterjee, 2007) represent the largest concentration of dicynodont fossils from the Upper Triassic of the southwestern U.S.A. outside of the *Placerias* Quarry (Camp & Welles, 1956). These dicynodont elements were collected from 1993 through 2014 and serve as the basis for the dicynodont described here, which is based in part on Mueller's (2016) dissertation.
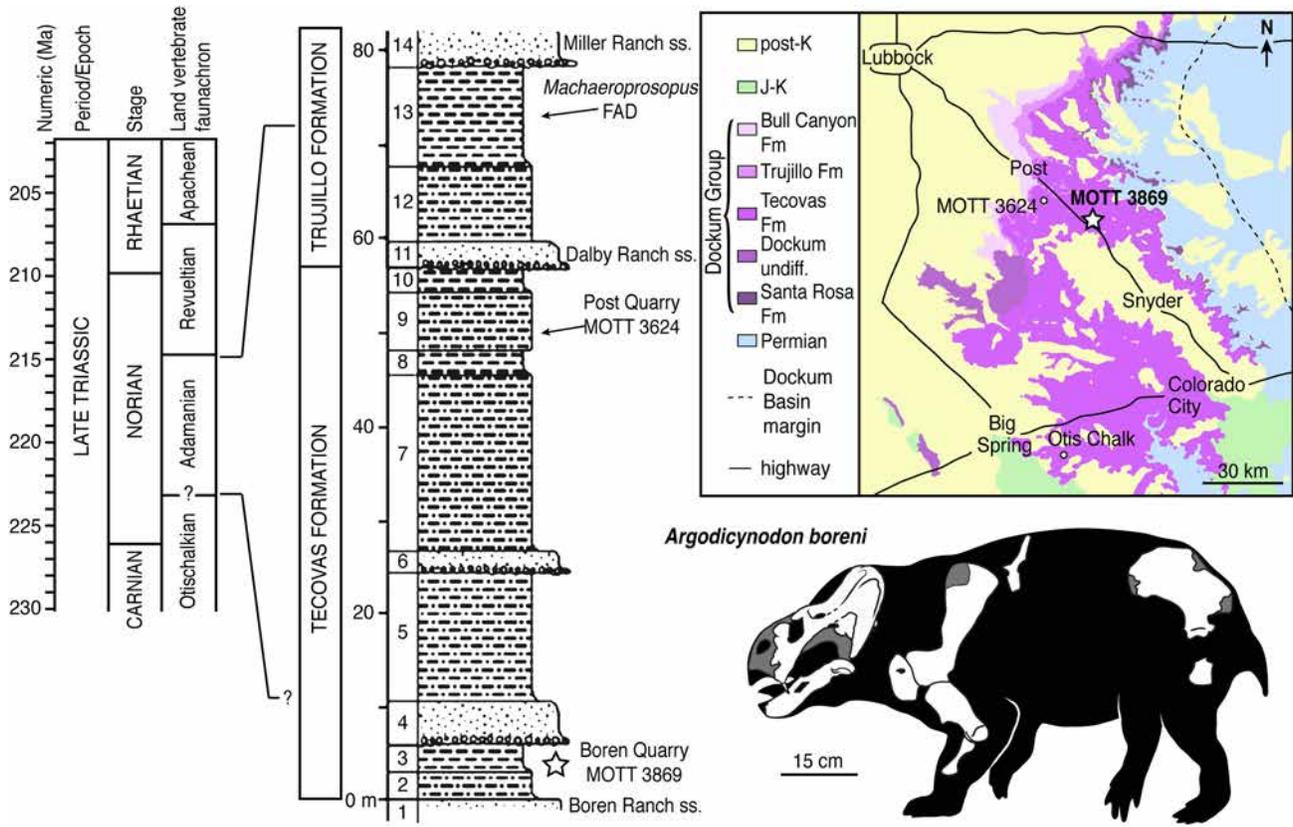
FIGURE 1. Location and stratigraphic position of the locality MOTT VPL 3869 (Boren Quarry) (white star) in Garza County, Texas, U.S.A. Local stratigraphic column is modified from Martz et al. (2013). Geologic map (inset) is modified from Mueller (2016). *Argodicynodon boreni* reconstruction (lower right) includes some elements that are flipped for comparison.

TABLE 2. Specimens and skeletal element(s) attributed to *Argodicynodon boreni* gen. et sp. nov. from MOTT VPL 3869 (Boren Quarry). Quarry locations are detailed in Mueller (2016).

Quarry location	Specimen	Element(s)
XVI (16)	TTU-P18107	partial skull roof
	TTU-P11869	ilium
XVII (17)	TTU-P10753	vertebrae
	TTU-P09421	mandible
XVIII (18)	TTU-P10407	tusk
	TTU-P19195	articular (right)
XXIII (23)	TTU-P10402 (holotype)	partial skull
	TTU-P11861	vertebra
	TTU-P11863	vertebra
XXIX (29)	TTU-P11871	distal humerus
XXXI (31)	TTU-P20042	humerus (left)
XXXIV (34)	TTU-P10751	proximal radius (left)
	TTU-P10752	squamosal
	TTU-P11150	distal radius (left)
	TTU-P19196	skull fragment
XXXV (35)	TTU-P11669	vertebra
XXXVIII (38)	TTU-P11870	scapulocoracoid (left)
VLI (41)	TTU-P12141	squamosal fragment
Unknown coordinate:	TTU-P16999	scapula
	TTU-P18108	pubis
	TTU-P11862	vertebra
	TTU-P10450	skull fragment
	TTU-P22384	skull fragment

TABLE 3. Boren Quarry faunal list (updated from Mueller, 2016).

Major clade	Taxon ID
Temnospondyli	*Buettnererpeton bakeri*
Dicynodontia	*Argodicynodon boreni* gen. et sp. nov.
Procolophonia	Procolophonidae incertae sedis
Drepanosauridae	Drepanosauridae incertae sedis
Tanystropheidae	cf. *Tanystropheus*
Azendohsauridae	*Malerisaurus langstoni*
	Azendohsauridae incertae sedis
Trilophosauridae	*Trilophosaurus buettneri*
	Trilophosaurus jacobsi
	Trilophosaurus dornorum
	Trilophosaurus incertae sedis
Doswelliidae	*Doswellia kaltenbachi*
	Vancleavea campi
Phytosauria	'Paleorhinus-grade' parasuchids
Aetosauria	*Calyptosuchus wellesi*
	Stagonolepididae incertae sedis
Paracrocodylomorpha	Paracrocodylomorpha incertae sedis
Poposauroidea	*Poposaurus gracilis*
	Shuvosaurus inexpectatus
Rauisuchidae	cf. *Postosuchus*
Crocodylomorpha	Crocodylomorpha incertae sedis
Dinosauromorpha	*Dromomeron gregorii*
	Theropoda incertae sedis

Institutional Abbreviations—**FMNH**, Field Museum of Natural History, Chicago, IL, U.S.A.; **MOTT VPL**, Museum of Texas Tech Vertebrate Paleontology locality; **NMMNH**, New Mexico Museum of Natural History and Science, Albuquerque, NM, U.S.A.; **TTU P**, Texas Tech University Paleontology Collections, Lubbock, TX, U.S.A.; **UCMP**, University of California

Museum of Paleontology, Berkeley, CA, U.S.A.; **USNM**, United States National Museum, Washington, DC, U.S.A.

MATERIALS AND METHODS

Geological Setting and Locality

All specimens of the new dicynodont, *Argodicynodon boreni* gen. et sp. nov., come from the Boren Quarry (MOTT VPL 3869) (Fig. 1, Table 2). The quarry is located in southeastern Garza County, Texas, U.S.A. Fossils from the Boren Quarry come from the lower strata of the Norian-aged Tecovas Formation (Dockum Group). The quarry site, a small erosional basin-like feature with an exhumed Triassic channel, is located on private land approximately 25 km southeast of the town of Post, Garza County, Texas (Fig. 1). A diverse fauna has been collected from the Boren Quarry. The identifications are preliminary and currently under study (Table 3).

Here, the term Tecovas Formation is applied to strata exposed at the Boren Quarry, as opposed to "correlative with the Tecovas Formation" or "lower Cooper Canyon" (Lessner et al., 2018; Martz, 2008; Martz et al., 2013). These formational names assumed validity of the Cooper Canyon Formation (Lehman et al., 1992). However, The Bull Canyon Formation (Lucas & Hunt, 1989) was given priority over the upper part of the Cooper Canyon Formation overlying the Trujillo and Tecovas Formations (Cather et al., 2013). The Boren Quarry is approximately 6 m above the base of the Tecovas Formation, which is defined as the contact with the top of the Boren Ranch Sandstone (Mueller, 2016). The top of the Tecovas Formation is capped by the Dalby Ranch Sandstone, which forms the base of the Trujillo Formation (Fig. 1). The base of the Trujillo Formation in Garza County was established by Mueller (2016) who traced the Trujillo Formation from Crosby County to Garza County. This places the Post Quarry near the top of the Tecovas Formation (Mueller, 2016).

Martz et al. (2013) and Lessner et al. (2018) place the vertebrate assemblage of the Boren Quarry in the Otischalkian Land Vertebrate Faunachron (LVF). Martz (2008) placed the FAD of *Paleorhinus* in Garza County at MOTT VPL 3867 about 15–18 m above the base of the Tecovas Formation. Another 'Paleorhinus-grade' phytosaur, *Wannia* (= *Paleorhinus*) *scurriensis*, occurs lower in the Dockum (Santa Rosa Formation) than the 'Paleorhinus-grade' phytosaur at MOTT VPL 3867 (Stocker, 2013). Martz (2008) pointed out that the FADs of the phytosaur taxa in the Dockum Group are questionable due to the small sample size. However, despite the small phytosaur sample size it appears that the Boren Quarry would most likely fall within the Otischalkian LVF based on these *Paleorhinus* occurrences and the associated assemblage.

Phylogenetic Methods

To evaluate the position of *Argodicynodon* within Kannemeyeriiformes, we conducted a phylogenetic analysis based on the dicynodont matrix of Szczygielski and Sulej (2023) (the matrix was originally adapted by these authors from Kammerer and Ordoñez, 2021). The matrix was updated to include character scores for the new taxon *Argodicynodon* and then two separate analyses were performed: (i) a parsimony analysis based on the full dataset encompassing Dicynodontia and (ii) a quality-controlled parsimony analysis excluding non-kannemeyeriiform dicynodont taxa and characters plus any fragmentary taxa having fewer than 50% of characters codable (see Appendix 1 and online supplemental dataset). For the first analysis, the resulting data matrix consisted of 23 continuous and 176 discrete (numeric) cranial and postcranial characters coded for 120 therapsid taxa (which included 103 dicynodonts). The therapsid

Biarmosuchus tener was used as the outgroup. Pre-existing character scores were mostly unchanged, although character 136, regarding the position of the angular reflected lamina and articular, was changed in *Placerias* to '?' due to mostly unassociated/disarticulated mandibular elements in that taxon. This calls into question the interpretation of the mandible in Cox (1965), which was significantly restored and modified from Camp and Welles (1956).

The analyses were performed in TNT 1.5 (Goloboff & Catalano, 2016) where the character sets were parsed into "continuous" and "numeric" partitions with continuous characters treated as additive following the method of Goloboff et al. (2006). For the full dicynodont dataset, a New Technology search was performed using default search parameters with 1000 initial addition sequence replicates to generate the most parsimonious trees. A second, revised matrix consisting of 29 taxa and 110 characters (23 continuous and 87 numeric) was also analyzed in TNT 1.5 following the same protocol described for the above analysis. The second analysis excluded kannemeyeriiform taxa scored for fewer than 50% of characters. Non-kannemeyeriiform taxa and uninformative characters with respect to Kannemeyeriiformes were also largely excluded to reduce analytical time, but the well-represented *Aulacephalodon bainii*, *Dicynodon angielczyki*, *Lystrosaurus declivis*, and *Lystrosaurus murrayi* were retained for outgroup comparisons.

SYSTEMATIC PALEONTOLOGY

SYNAPSIDA Osborn, 1903
THERAPSIDA Broom, 1905
DICYNODONTIA Owen, 1859
KANNEMEYERIIFORMES Maisch, 2001
STAHLECKERIIDAE Cox, 1965
PLACERIINAE King, 1988
ARGODICYNODON BORENI, gen. et sp. nov.
(Figs. 2–9)

Etymology—The genus-species combination translates to "Boren's swift dicynodont." The genus name uses the Greek "*argos*" (meaning "swift" or "quick") which is also a reference to *The Argo*, the mythological ship that Jason and the Argonauts sailed to find the Golden Fleece. This is combined with the Neo-Latin suffix "*dicynodon*" (meaning "two dog-tooth") in reference to the taxon's dicynodont affinities. The species name honors John Boren and family who owned the ranch property when the quarry was discovered.

Holotype—TTU-P10402, a partial skull, approximately 50% complete and consisting of the right maxilla with partial tusk, right circumorbital bones, intertemporal region with intact skull roofing elements, the right and left disarticulated squamosals, and an incompletely preserved braincase (Figs. 2, 3).

Referred Specimens—Partial skull roof, TTU-P18107; skull roof fragments, TTU-P10450, TTU-P19196, TTU-P22384; partial tusk, TTU-P10407; squamosals, TTU-P10752, TTU-P11292, TTU-P12141; mandible (complete with left and right rami), TTU-P09421; right articular, TTU-P19195; vertebrae, TTUP10753, TTU-P11669, TTU-P11861, TTU-P11862, TTU-P11863; left scapulocoracoid (complete), TTU-P11870; partial scapula, TTU-P16999; left humerus, TTU-P20042; incomplete distal humerus, TTU-P11871; incomplete left radial elements (proximal and distal), TTU-P10751, TTU-P11150; left ilium, TTU-P11869; and left pubis, TTU-P18108 (Table 2).

Locality and Horizon—All specimens are from the Boren Quarry (MOTT VPL 3869) in Garza County, Texas, U.S.A. (Fig. 1). Based on the stratigraphic position of the locality within the lower strata of the Triassic Tecovas Formation (Dockum Group), in combination with its associated vertebrate
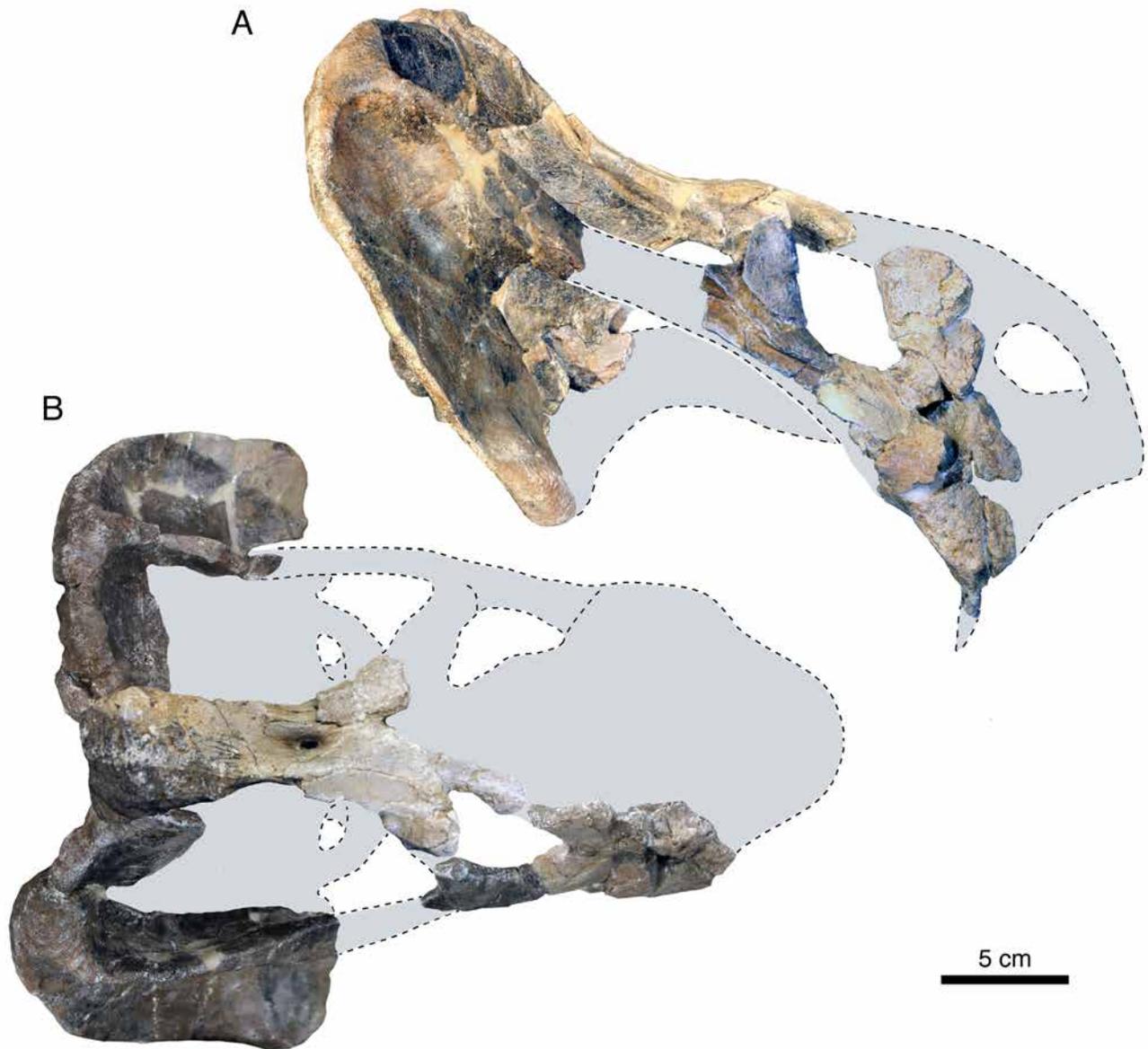
FIGURE 2. Holotypic skull of *Argodicynodon boreni* gen. et sp. nov., TTU-P10402: photograph of reconstructed skull in right lateral (**A**) and dorsal (**B**) views.

assemblage, the site is interpreted as early Norian in age (Otischalkian LVF) (Martz, 2008; Martz et al., 2013). Detailed locality information, coordinates, and quarry maps are archived in the Museum of Texas Tech, Lubbock, which are available to qualified researchers on request.

Diagnosis—Mid-sized kannemeyeriiform (skull length ~33–49 cm) apomorphic in having an interparietal with broad, interdigitating sutural contacts with the squamosals; skull narrower than *Placerias*; basal tubers low and closely spaced near the midline, with only shallow notch separating them from each other and from the mastoid (in *Placerias*, the tubers are extended ventrally with wide separation from midline, oriented ventrolaterally, and with a deeply incised lateral notch separating the auditory structure from the mastoid); caniniform process of the maxilla is dorsoventrally deep and well developed; tall, narrow intertemporal region formed by the parietals with long postorbitals forming the lateral faces of the dorsal platform; interparietal forms knobby, bilobed exostoses that wedge in between the

parietals to form a W-shaped outline in dorsal view; posterior sulcus present along the sagittal plane of interparietal divides each lobe; elongate preparietals and frontals extend posteriorly beyond the anteroposteriorly elongated pineal foramen, extensively engulfing it; the basioccipital and exoccipital portions of the occipital condyle are distinct, and the dorsal fossa separating the left and right exoccipitals is deeply incised and dorsoventrally deep; articular bears a tab-like medial flange, massive and tongue-shaped, that is autapomorphic in its proportionately larger size than the lateral saddle for the quadrate (proportions are the inverse in *Placerias* and other stahleckeriids).

Further differs from the contemporary placeriines *Placerias hesternus* and *Moghreberia nmachouensis* in the following combination of primitive and apomorphic characters: sutural surface for premaxilla borders directly on the maxillary canine alveolus rather than being anterodorsally separated from the alveolus by substantial bone; frontal borders the orbit only via a narrow process on the posteriormost corner of the orbital rim, narrowly
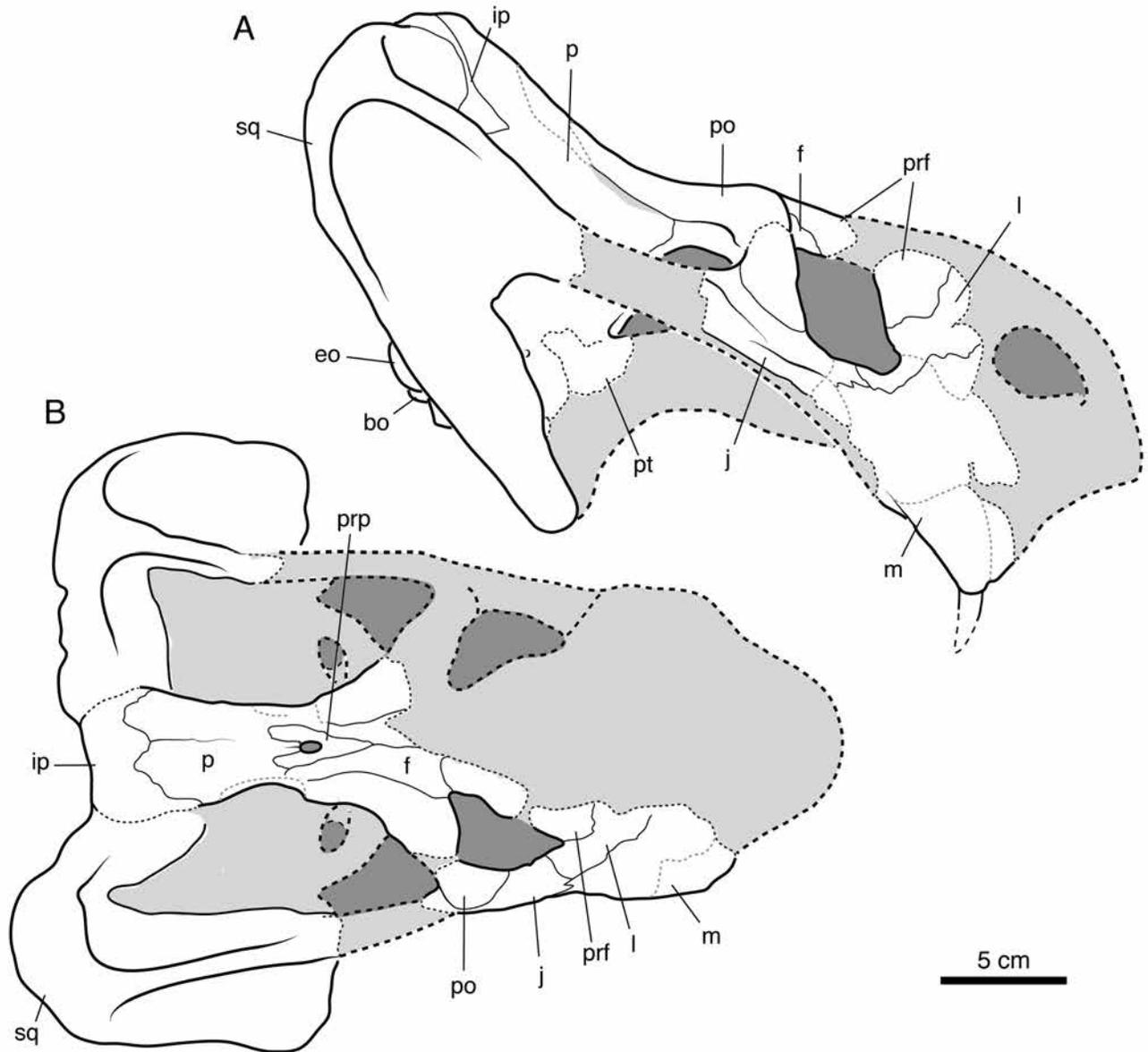
FIGURE 3. Holotypic skull of *Argodicynodon boreni* gen. et sp. nov., TTU-P10402: line drawings in right lateral (**A**) and dorsal (**B**) views with individual elements labeled. **Abbreviations**: **bo**, basioccipital; **eo**, exoccipital; **f**, frontal; **ip**, interparietal (= postparietal); **j**, jugal; **l**, lacrimal; **m**, maxilla; **p**, parietal; **po**, postorbital; **prf**, prefrontal; **prp**, preparietal; **pt**, pterygoid; **sq**, squamosal.

separating the prefrontal and postorbital (shared in some shansiodontids, kannemeyeriids, and stahleckeriines); small, oval parietal foramen; fenestra ovalis faces mostly ventral rather than laterally as in *Placerias*; dentary median groove near symphysis is proportionally narrower than in either *Placerias* or *Moghreberia* and surrounded by a wider dorsal dentary table. Differs from *Placerias* but shares with *Moghreberia*: maxillary anterior pit absent (also absent in *Zambiasaurus*) palatal face of maxilla is instead smooth and flat; preparietal present and depressed instead of flush with skull roof (also in *Pentasaurus*); tusk visible in lateral aspect (not covered by bony plate and protruding below the ventral aspect of the caniniform process) but gracile and diminutive in diameter.

Comments—*Argodicynodon* is represented by multiple subadult to adult individuals. An adult specimen, represented by a mandible, is estimated to have a skull length of up to 49 cm, while a subadult specimen, represented by a partial skull, is estimated to have a skull length of only 33 cm. All of the specimens come from approximately the same stratigraphic level in the quarry. However, they are laterally dispersed within this horizon over an area of up to 300 m (Mueller, 2016:fig. 1.4). The minimum number of individuals is eight in the present collection, based on the number of disassociated skull or partial skull elements, although there may have been more based on the wide dispersal of elements within the quarry.

DESCRIPTION

Cranium

General—The overall character of the skull can be inferred from two specimens, including the greater portions of a skull designated as the holotype, TTU-P10402 (Figs. 2, 3), and a partial skull roof slightly larger in size, but preserving only the
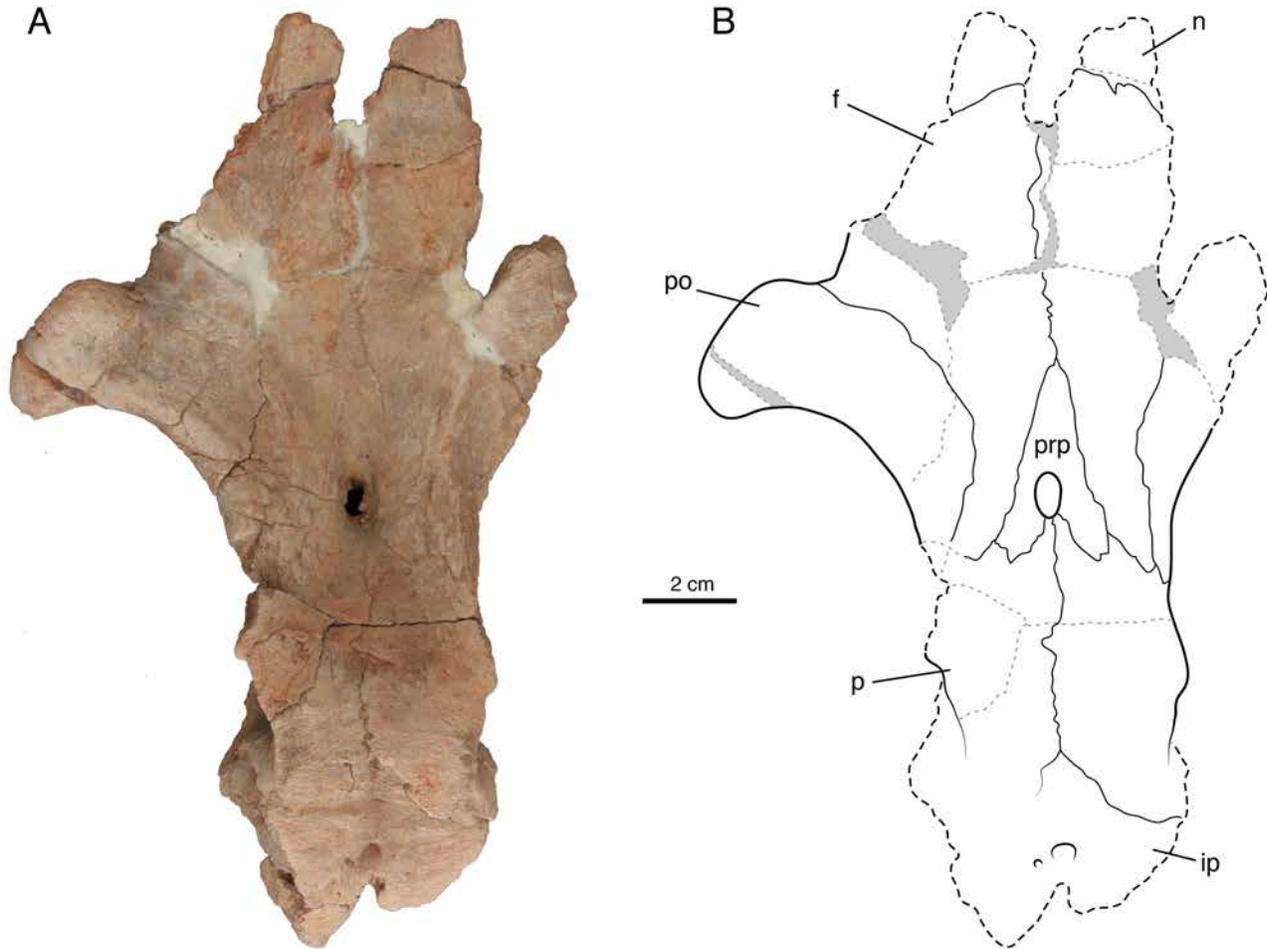
FIGURE 4. Referred skull roof of *Argodicynodon boreni* gen. et sp. nov., TTU-P18107 in dorsal view: photograph (**A**) and weighted line drawing (**B**). **Abbreviations**: **f**, frontal; **ip**, interparietal (= postparietal); **n**, nasal; **p**, parietal; **po**, postorbital; **prp**, preparietal.

dorsal interorbital and intertemporal regions, TTU-P18107 (Fig. 4). TTU-P10402 consists of both squamosals, the dorsoposterior portion of the skull, part of the right side of the skull, including the circumorbital bones, and part of the braincase. Description of the cranial elements below is largely based on this skull, which is interpreted as a subadult having an estimated skull length of 33 cm and approximately 19 cm at its greatest width between the squamosals (suggesting a proportionately narrower skull than that of *Placerias*; Cox, 1965:fig. 26). The palate, naris, and premaxillae are not preserved. TTU-P18107 consists of a partial skull roof, larger than TTU-P10402, with a flat intertemporal region and the same configuration of bones around the pineal foramen. The preparietal, for example, wraps around and extends posterior to the pineal foramen as in TTU-P10402. Both specimens suggest a tall intertemporal region that rises well above the dorsal limits of the orbits. The maximum width of the interparietal on the dorsal skull table is 54 mm in TTU-P18107 compared with 44 mm in TTU-P10402. The pineal foramen of TTU-P18107 is slightly larger (13 mm) than in TTU-P10402 (10 mm). The length of the intertemporal region from the anterior margin of the pineal foramen to the occiput is 112 mm in TTU-P18107 and 97 mm in TTU-P10402.

Skull Roof—Though portions of the snout are missing, including the premaxilla and septomaxilla, the skull roof can be reconstructed as relatively [anteroposteriorly] short and [dorsoventrally] tall based on the deep maxilla and high intertemporal platform rising well above the orbits in TTU-P10402

(Figs. 2, 3). The caniniform process is offset ventrolaterally from the rest of the skull, forming a shallow embayment along its anterolateral face. The caniniform process is thick and triangular in ventral cross section rather than forming a mediolaterally compressed flange. The caniniform process is also dorsoventrally deep and extends ventrally well below the skull, but bears a proportionally small tusk as is sometimes encountered in stahleckeriids. The maxilla extends posteriorly toward the level of the posterior limit of the orbit, overlapping the jugal substantially based on deep facets scoured ventrally on the jugal along the suborbital bar where the maxilla would have sutured (Fig. 3A). Although this posterior portion of the maxilla is broken away in TTU-P10402, the maxilla clearly extended posteriorly to contact the squamosal directly beneath the postorbital bar, based on their impressions on the jugal.

Implanted within the thick, triangular caniniform process, a slender tusk is present, protruding below the ventral aspect of the caniniform process, but extremely diminutive in diameter. The moderate development of the tusk differs from the more vestigial tusks of *Placerias* which barely protrude from the inner margin of the maxillary process and are laterally obscured by bone. In *Argodicynodon*, the premaxilla-maxilla suture, which is serrate, rests on the anterior edge of the canine alveolus so that there would be no substantial precanine lamina of the maxilla or bony coverings. The tusk in the right maxilla of TTU-P10402 is fractured; however, it is tapered and there is no evidence of wear facets. The tusk is also gently curved posteriorly. A slightly
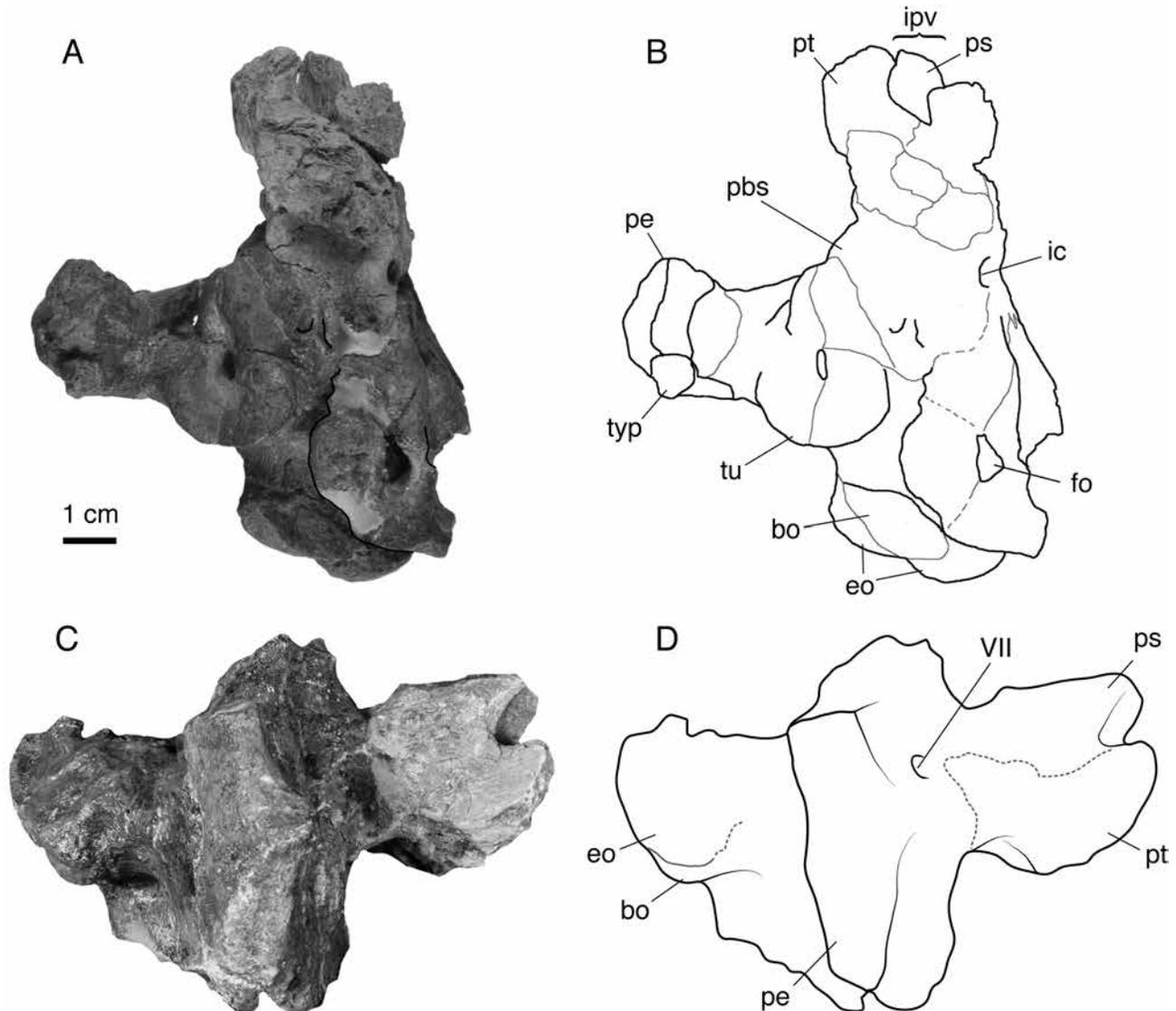
FIGURE 5. Braincase of *Argodicynodon boreni* gen. et sp. nov., TTU-P10402 in ventral (**A**, **B**) and right lateral (**C**, **D**) views. **Abbreviations**: **bo**, basioccipital; **eo**, exoccipital; **fo**, fenestra ovalis; **ic**, internal carotid foramen; **ipv**, interpterygoid vacuity; **pbs**, parabasisphenoid basal plate; **pe**, periotic; **ps**, parasphenoid anterior process; **pt**, pterygoid; **tu**, basal tubera; **typ**, tympanic process; **VII**, foramen for facial nerve.

larger, isolated tusk, TTU-P10407, is broken on both the proximal and distal ends, but also shows no wear facets. The broken sections show the dense internal structure of the dentin and lack of enamel typical of mature dicynodont tusks (Green, 2009, 2012; Whitney et al., 2021). It is slightly flattened on the posteromedial margin, forming a slight ridge towards the posterior edge. The slight curvature and shape of the tusk indicates that the tusk was from the right maxilla.

The nasals are not preserved well enough for description, though small portions may be preserved in TTU-P18107 on the left and right sides (Fig. 4). The lightly pitted texture on the dorsal surface of the nasals suggests that the keratinous rhamphotheca could have covered a substantial portion of the nasal region.

The circumorbital bones include the prefrontal, frontal, postorbital, jugal, and lacrimal, with the frontal only narrowly participating on the roof of the orbit. In TTU-P10402, the prefrontal is just a small fragment attached to the lacrimal anterolaterally. Most of the dorsal and anteromedial portions are broken away. The lacrimal is preserved as a small, irregularly shaped fragment

on the right side of the skull in TTU-P10402 where it is shown to form the anterolateral limit of the orbit (Figs. 2, 3). Dorsally on the skull table, the narrow frontals project posteriorly alongside the preparietal which in turn wedges between the frontals. Unlike in *Placerias*, the frontals do not form part of the wall of the pineal foramen, as they are well separated by lateral flanges of the preparietal. The posterior processes of the frontals extend only slightly posterior to the pineal foramen to about the posterior edge of the preparietal which envelops the foramen. The dorsal surface of the frontal is broadly convex over the post-orbital bar and orbits (rather than the concave condition in *Placerias*; Kammerer et al., 2013:fig. 1) and indicates the restored interorbital region would have been slightly curved or domed in lateral view and not flat.

The jugal in TTU-P10402 bears a sutural surface where the squamosal overlapped its lateral surface anteriorly to where the squamosal made contact with the maxilla, overlapping the jugal ventrally beneath the postorbital bar (Figs. 2A, 3A). A small strip of the jugal would have been exposed laterally on the cheek, narrowly separating the postorbital from direct
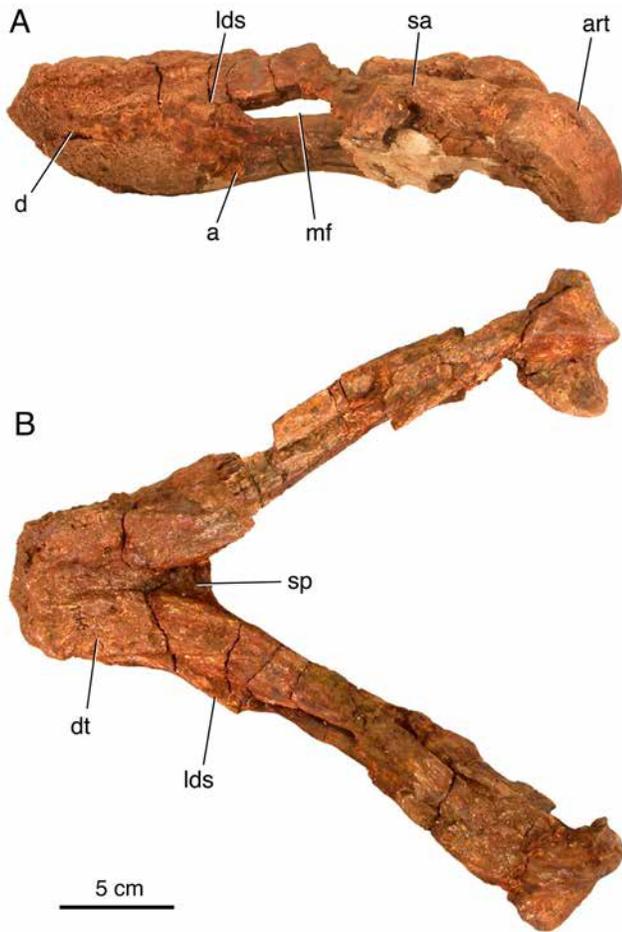
FIGURE 6. Mandible of *Argodicynodon boreni* gen. et sp. nov., TTU-P09421 in left lateral (**A**) and dorsal (**B**) views. **Abbreviations**: **a**, angular; **art**, articular; **d**, dentary; **dt**, dentary table; **lds**, lateral dentary shelf; **mf**, mandibular fenestra; **sa**, surangular; **sp**, splenial.

FIGURE 7. Dorsal vertebra of *Argodicynodon boreni* gen. et sp. nov., TTU-P10753 in anterior (**A**) and left lateral (**B**) views.

contact with the squamosal or maxilla (similar to *Placerias* but unlike in *Stahleckeria*, for example, where these bones form a sutural junction beneath the orbit and cover the jugal; Kammerer & Ordoñez, 2021:fig. 20; Maisch, 2001:fig. 2). The jugal projects anterodorsally to contact the lacrimal but it is broken away posteriorly in TTU-P10402.

The postorbital forms the lateral margin of the intertemporal platform projecting along and parallel to the frontal and parietal. Its jugal process is long, forming a thickened bar that completely bounds the orbit posterolaterally, and bears a rugose surface texture roughened by exostoses as in the majority of non-shansiodontid kannemeyeriiforms (stahleckeriids and kannemeyeriids). The process overlaps the jugal substantially and forms the entire posterior margin of the orbit. The very long posterior process of the postorbital is flat and smooth by contrast, and forms a broadly concave surface along the lateral face of the temporal fossa that would have been covered by jaw adductor muscles. Although the posterior limit is broken in TTU-P10402, the sutural facet for the posterior process can be seen etched into the parietal on the right side of the skull (Figs. 2A, 3A), confirming the long posterior extent of this process. It is therefore interpreted as a long strap-like element rather than the foreshortened quadrangular postorbital that is more typical of *Placerias* (Cox, 1969:figs. 26, 28). Due to its length, the posterior process would have nearly contacted the interparietal.
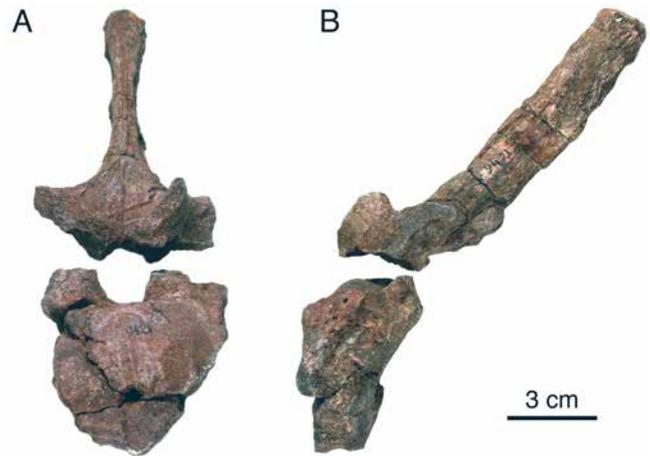
Behind the interorbital region, the tall, narrow intertemporal region rises at a steep angle (Figs. 2A, 3A), a feature that variably occurs in *Rabidosaurus* and some other kannemeyeriids, but also in *Ischigualastia*, *Placerias*, and *Moghreberia* among stahleckeriids (Dutuit, 1980; Olivier, 2020). In other respects, the configuration of bones of the posterior skull roof is apomorphic in *Argodicynodon*, differing from other kannemeyeriiforms (Camp & Welles, 1956; Cox, 1965; Maisch, 2001). The intertemporal region forms a moderately narrow 'bar' and is formed by the parietals with elongated postorbitals along its lateral faces. A median preparietal element is present, which is anteroposteriorly elongated and transversely narrow. It forms a projection anteriorly between the frontal midline suture, then sweeps backwards along the pineal foramen and projects posteriorly just beyond the pineal foramen to about the same point where the frontals terminate. The posterolateral flanges of the preparietal form almost the entire wall of the pineal foramen with the parietal extending anteriorly forming the floor of the posterior groove of the pineal foramen. This configuration resembles that described in a specimen of '*Rechnisaurus*' by Cox (1991:fig. 2) although the posterior margins are not preserved in that specimen. The pineal foramen of *Argodicynodon* is transversely narrow and forms a groove-like dorsal depression that shallows posteriorly. The pineal foramen in TTU-P10402, where it is best preserved, is 5.7 mm in width and 10.7 mm in length. The posterior groove is approximately 40.6 mm long.

Posterior to the pineal foramen, the parietals form the intertemporal platform of the skull. The intertemporal platform is moderately narrow (approximately 43 mm wide in TTU-P10402). However, it is relatively flat posteriorly and slightly concave anteriorly towards the pineal foramen at its flexure with the frontal. The contact of the parietals with the frontals is posterior to the pineal foramen. The parietals form a groove leading anteriorly to contact the pineal foramen. The interparietal forms an ovoid, bulbous knob at the dorsoposterior extent of the intertemporal region with a W-shaped sutural connection to the parietal superficially similar to *Dolichuranus*, *Sangusaurus*, and *Wadiasaurus* (Angielczyk et al., 2017; Damiani et al., 2007). The interparietal faces mostly posteriorly where it bears thickened bilobed exostoses on the occipital face. There is a small vertical groove along the posteroventral plane of the interparietal. On the posterolateral margins, the interparietal forms a "tongue and groove" articulation with the squamosals. The interparietal projects anteriorly both at the midline of the skull and along the lateral margin of the parietals (Figs. 2B, 3B). This
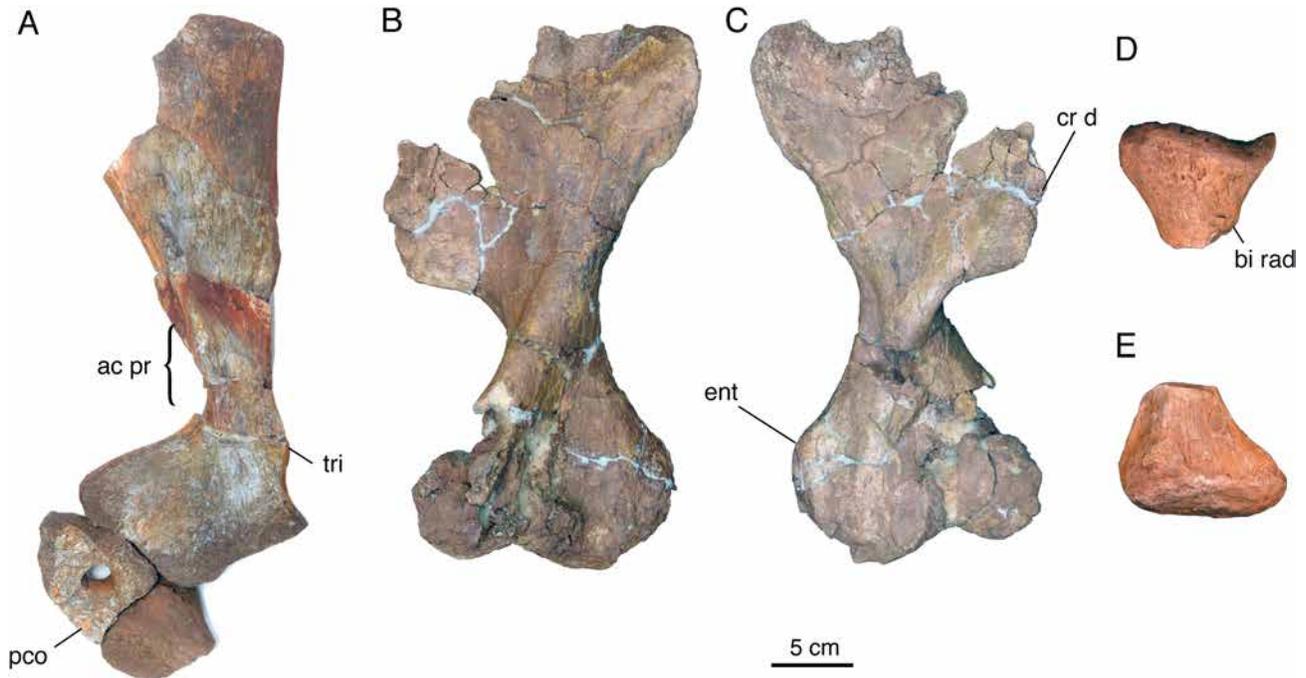
FIGURE 8. Forelimb elements of *Argodicynodon boreni* gen. et sp. nov. **A**, left scapulocoracoid, TTU-P11870 in lateral view; **B**, left humerus, TTU-P20042 in anterior view; **C**, same as '**B**' in posterior view; **D**, proximal left radius, TTU-P10751 in posterior view; **E**, distal left radius, TTU-P11150 in posterior view. Elements are shown to scale. **Abbreviations**: **ac pr**, broken area for acromion process; **bi rad**, tubercle for biceps radialis; **cr d**, delto-pectoral crest, **ent**, entepicondyle; **pco**, procoracoid; **tri**, triceps tubercle.
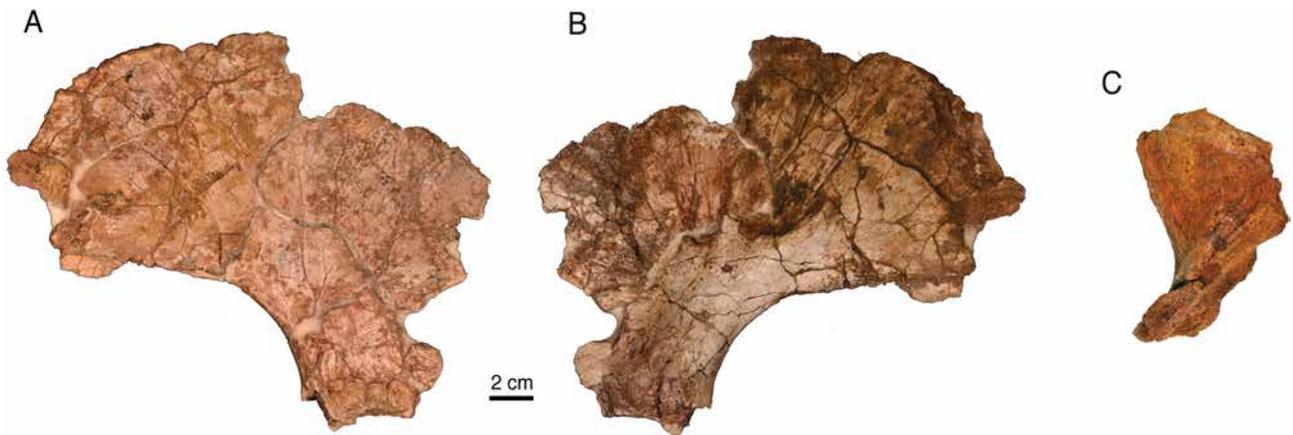
FIGURE 9. Pelvic elements of *Argodicynodon boreni* gen. et sp. nov. Left ilium TTU-P11869 in (**A**) lateral and (**B**) medial views. Left pubis TTU-P18108 in lateral view (**C**).

configuration differentiates *Argodicynodon* from *Stahleckeria*, *Kannemeyeria*, and *Placerias*, but a broad overlap is also seen in *Wadiasaurus* (Bandyopadhyay, 1988).

Multiple squamosal specimens are represented for *Argodicynodon*, including both the left and right in the holotype TTU-P10402. The squamosal of TTU-P10402 is only 226 mm in height from the dorsal transverse crest to the ventral margin of the quadrate process. The dorsal transverse crest is rugose and has a maximum thickness of 33.9 mm. The confluence between its three rami is also thickened and rugose, though not as extremely thickened as that of some large *Placerias* specimens (e.g., UCMP 137369). The jugal process of the squamosal is broken away on both sides. The squamosals are each approximately

70 mm wide at the dorsal margin of the lateral fossa for the mandibulae adductor externus. The adductor fossa also has a strong vertical orientation as interpreted in *Placerias* (Cox, 1965:fig. 28). Just dorsal to the articular surface for the quadrate, the squamosal's descending process is 63.8 mm wide and 6.5 mm thick. Dorsally, the squamosal articulates broadly with the interparietal via an interdigitating suture. A more massive right squamosal, TTU-P10752 (Table 2), was found alongside additional skull fragments, but it is still much smaller than the squamosal in adult *Placerias*, thus distinguishing *Argodicynodon* in its proportions and smaller size.

Palate, Splanchnocranium, and Suspensorium—Very little of the palate of *Argodicynodon* is preserved, limiting any

description of the palatal view or adjoining splanchnocranium at present. Nevertheless, portions of the pterygoid and a portion of parasphenoid between the interpterygoid vacuity are visible in the holotype TTU-P10402 in ventral view (Fig. 5). A small portion of the left and right pterygoid extends posteriorly and forms a midline suture just behind the interpterygoid vacuity. Although there is some cracking and desiccation of these elements in the *Argodicynodon* holotype, they appear slightly thickened and may have formed curved processes where they joined to the parabasisphenoid behind the interpterygoid vacuity. A strongly curved ridge on the pterygoid processes is seen in ventral view in '*Rechnisaurus*' (Cox, 1991:fig. 3E) but a similar thickened ridge may also be present in *Placerias* (e.g., UCMP 32458). This posterior region, however, is badly crushed in *Argodicynodon* and partly broken away and the anterior rami of the pterygoids are completely missing. The epipterygoid is also missing. The sutures between the parabasisphenoid and pterygoid are obscured by the crushed pterygoid.

Braincase and Occiput—The braincase is preserved in TTU-P10402 (Fig. 5), though it is incomplete and distorted. Preserved portions include: parabasisphenoid, periotics, basioccipital, and the left and right exoccipitals contributing to the occipital condyle. Ventrally the parabasisphenoid contacts the anterior margin of the prootic. It extends anteriorly to contact the pterygoids. Dorsally the parabasisphenoid forms the floor of the braincase. The anterior process extends anteriorly only a short distance in between and dorsal to the interpterygoid vacuity, as is typical in stahleckeriids, before being broken away in the specimen. Posterolaterally, there is a large carotid foramen. Ventromedially, paired shallow depressions occupy the basal plate just anterior to the basioccipital and basal tubera.

The periotics are formed by thick, dense bony contributions from the prootic and opisthotic elements, although sutural separations are difficult to identify, suggesting these were fused into a single periotic ossification (Olson, 1944) in TTU-P10402 (Fig. 5). The prootic portion is broken laterally, but can be seen in front of the opisthotic bounding the anterior portion of the fenestra ovalis and continuing anteriorly toward the pterygoid. Anterodorsally, in front of the paroccipital process, there is a small facial foramen (VII) facing anteriorly. The prootics nearly join ventromedially, broadly overlapping the basioccipital posteriorly and overlapped by the basisphenoid anteriorly. The opisthotic contacts the basioccipital medially and its posterolateral (paroccipital) processes are broken away on both sides of the skull. The opisthotic forms the posterolateral portions of the basal tubera which surround the fenestra ovalis. The basal tubera are low and closely spaced near the midline, with only a shallow notch separating them laterally from the mastoid portion of the paroccipital processes ("tympanic process" of Cox, 1959). In *Placerias*, the tubera are extended ventrally with wide separation from the midline, oriented ventrolaterally, and bear a deeply incised lateral notch separating the auditory structure from the mastoid. In this respect, the size of the tubers and paroccipital processes and their spacing more closely resemble *Dolichuranus* (a conservative kannemeyeriid; e.g., Damiani et al., 2007:fig. 3), *Ischigualastia* and *Dinodontosaurus* (Cox, 1965:figs. 2, 12) than other placeriines. Consequently, the fenestra ovalis also faces mostly ventral in *Argodicynodon*.

The occipital condyle is tripartite. The basioccipital and exoccipital contributions to the condyle are distinct, and the dorsal fossa separating the left and right exoccipitals is deeply incised and dorsoventrally deep. The basioccipital forms the ventral third of the occipital condyle and in TTU-P10402 has a maximum condylar width of 19.5 mm. The basioccipital extends anteriorly to form part of the ventral surface of the braincase contacting the basisphenoid. Ventrally the basioccipital forms the depression between the basal tubera and its paired ventral processes form the posteromedial portion of the basal tubera.

The exoccipitals join immediately above and to the sides of the basioccipital forming the dorsal portion of the occipital condyle. Their wide separation in TTU-P10402 suggests that the exoccipital does not fully fuse in *Argodicynodon* or reflects its status as a subadult specimen. However, even in comparatively small specimens of *Placerias* the exoccipitals are well fused (e.g., UCMP 26680; Camp & Welles, 1956). On the right side of TTU-P10402, there is a groove where the hypoglossal foramen (XII) would have been if most of the bone was not broken away. Anterolaterally, the exoccipitals join with the paroccipital processes.

Mandible

A single mandible, TTU-P09421, is described here. The mandible is mostly complete but weathered into numerous fragments that have been reconstituted during fossil preparation (Fig. 6). The mandible is estimated to be over 30% larger than would be expected for the holotypic skull TTU-P10402. The mandible is approximately 325 mm in length from the anterior limit of the dentary to the articular. The mandible is 353 mm wide from the lateral margins of the left articular to the right.

Dentary—As in all dicynodontoids, the dentary is edentulous with an anterior 'beak' that in life would have been covered by a keratinous rhamphotheca. The anteriormost tip of the dentary in TTU-P09421 is slightly broken away. However, the morphology indicates that it formed an upturned but rather blunt beak. There is a dorsal median groove (Cox, 1998) in the dentary along the posterior two thirds of the symphysis, extending anteriorly for 37 mm. The groove is bounded laterally by the tall, flat lingual ridges of the dentary table ('dentary pads' of Cox, 1998), and there is the base of a blade-like medial projection that is broken away. The median groove is proportionately narrow compared with the wide bounding table or 'pads.' The dentary is dorsoventrally shallow and is shallowest at midlength, being only 71.9 mm in height. The dentary extends posteriorly forming the dorsal portion of the jaw above the splenial and the portion of the jaw lateral to the splenial. A posterior dentary sulcus is present (Fig. 6). The dentary forms the dorsal margin of the mandibular fenestra, just behind the lateral dentary shelf, and continues posterodorsally toward its contact with the surangular.

The mandibular fenestra is smaller and shallower (more slit-like) than that of *Placerias*. The fenestra is 19 mm in height, but is 51 mm in length. The margins of the mandibular fenestra are formed by the splenial anteromedially, the dentary anterodorsally and laterally, and the surangular posterodorsally. The posteroventral margin of the mandibular fenestra is formed by the prearticular medially and the angular medially.

Splenial—The splenial is relatively narrow and projects anteriorly along the symphysis of the ventral portion of the jaw. The splenial forms the ventral floor of the sulcus. Medially the splenial extends posteriorly to the anterior limit of the mandibular fenestra. The dentary extends posteriorly at the anterior limit of the mandibular fenestra and the ventral margin of the splenial angles dorsally with the posterior limit of the splenial reaching to the posterior third of the mandibular fenestra.

Angular—The angular forms the lateral and ventral portion of the mandible extending from the dentary posteriorly to the surangular.

Surangular—The surangular is bordered by the dentary anteriorly, angular laterally, prearticular medially and ventrally, and the articular posteriorly.

Prearticular—The prearticular is a strap-like element that extends from the splenial anteriorly on the medial portion of the jaw posteriorly to the articular.

Articular—The articular is relatively short anteroposteriorly. The medial articular process is tab-like and is conspicuously

wider than the lateral articular surface. The right articular is 40 mm wide from the medial articular ridge to the lateral edge of the articular, and the left articular is 35 mm wide from the medial articular ridge to the lateral edge. The medial process is tab-like and is characteristically wide and gracile. The retroarticular process is not well preserved.

Postcrania

Vertebrae—A vertebra, a neural arch, and vertebral fragments TTU-P10753 (Fig. 7) were collected from the same quarry area as the mandible TTU-P09421. The vertebra and fragments are badly weathered. It is unknown if the most complete neural arch goes with the most complete centrum, although the centrum and neural arch are both from the anterior dorsal region. The margins of the centrum are abraded where the parapophysis and diapophysis should be. The vertebral canal is approximately one-third the width of the centrum. The centrum is 56 mm in height and estimated to be 60 mm in width. The centrum appears to be short, its anteroposterior length being approximately two-thirds the width of the centrum. The most complete neural arch has a neural spine that is tall, thin, and slightly posteriorly reclined (Fig. 7). It is 115 mm from the base of the postzygapophysis to the top of the neural spine. The neural spine has a small prespinous lamina, while the posterior edge is weathered away. There is a transverse expansion at the top of the neural spine reaching approximately 75% of the anterior-posterior length of the neural spine at its apex. The postzygapophysis is small and ventrolaterally directed. The prezygapophysis is relatively large, dorsomedially directed, and concave.

Scapulocoracoid—The pectoral girdle is best represented by a left scapula, coracoid, and procoracoid TTU-P11870 (Fig. 8A). The total dorsoventral height of the scapula is 369 mm, the anteroposterior length is 146 mm, and the narrowest anteroposterior length of the shaft of the scapula is 46 mm. The thickness across the glenoid is 56 mm. The triceps tubercle is a prominent, mound-like dome 42.1 mm in height and 20.3 mm in width. The tubercle is less prominent than in *Jachaleria*, but more prominent than that of *Eubrachiosaurus*, *Kannemeyeria*, *Placerias*, *Zambiasaurus*, and *Woznikella* (Szcygielski & Sulej, 2023). An acromion process was present in life, but largely broken away in the specimen. The anterior edge of the scapular blade has a concave depression formed partially by the scapular spine. The posterior margin of the scapular blade has a convex section beginning 141 mm dorsal to the glenoid and extending 124 mm dorsally. A second partial right scapula, TTU-P16999, is larger than the first (196 mm anteroposterior length) (Table 2), but is not as well preserved. As in kannemeyeriids and rarely in stahleckeriids like *Woznikella*, the ratio of the scapula proximal breadth relative to its length is extremely narrow (less than 0.4) (e.g., *Kannemeyeria simocephalus*, *Wadiasaurus*). As in *Woznikella*, the scapular blade narrows toward the level of the acromion where it forms a constricted 'neck-like' region (Szcygielski & Sulej, 2023:fig. 11), but differing markedly from *Placerias* in this regard. Likewise, the scapula of *Argodicynodon* is smaller and more gracile than that of *Placerias* and those from other Dockum Group localities (MOTT VPL 3867; Table 4).

The coracoid is interpreted as having an anterior-posterior length of 56.9 mm, although it is slightly damaged and preserves mainly the glenoid region. The procoracoid is 83.2 mm in length. The large procoracoid foramen, which is completely enclosed within the procoracoid, is 15.3 mm in height and had a groove projecting anteriorly for 25.7 mm. The dorsolateral, ventral, and posterodorsal margins of the bone are slightly abraded.

Humerus—A left humerus, TTU-P20042, is 326 mm in length and is nearly complete, missing only portions of the proximal head and proximal portions of the deltopectoral crest (Fig. 8B, C). The entepicondyle is more developed than that of *Eubrachiosaurus browni* or *Placerias hesternus* (Kammerer et al., 2013:fig. 5). It is similar in size to that of *Ischigualastia jenseni* and *Xiyukannemeyeria brevirostris*. The distal margin of the deltopectoral crest extends less perpendicular to the shaft in TTU-P20042 than in *Eubrachiosaurus browni*, *Ischigualastia jenseni*, and *Xiyukannemeyeria brevirostris* where it is solidly perpendicular. The ectepicondyle is less robustly developed in TTU-P20042 than in *Eubrachiosaurus browni* and *Placerias hesternus*.

Radius—Only pieces of the radius are preserved, including proximal (TTU-P10752) and distal (TTU-P11150) ends of a left radius that may have been associated. Both were collected in the same drainage six meters downstream from the squamosal TTU-P10752 (Table 2). The greatest width of the proximal end of the radius is 93 mm. The articular surface forms a shallow anterolateral dipping depression. The medial edge of the articular surface forms a sharp ridge subequal in height to the lateral margin. The facet that articulates with the ulnar trochlea on the humerus forms approximately one-third of the posterior articular margin forming a prominent lip just above the insertion tubercle for the biceps radialis. The specimen is broken at the proximal margin of the biceps radialis tubercle. The greatest width of the distal radius TTU-P11150 is 114 mm. This is slightly larger than the size of the radii of *Placerias* (Camp & Welles, 1956). The preserved portion of the distal radius is 84 mm in length. At the break, the shaft is 34 mm anteroposteriorly and approximately 50 mm mediolaterally. The articular surface forms a convex surface both anteroposteriorly and mediolaterally. The posterior two-thirds of the articular surface is inclined dorsally and is visible in the posterior view. Approximately one-third of the articular surface is visible in the anterior view. At the dorsal margin of the articular surface on the anterior face, near the lateral margin is a distinct groove projecting medially. The groove is 8 mm wide and reaches to the midline of the radius. In distal view, the articular surface narrows medially forming somewhat of a teardrop shape. If the distal and proximal ends belonged to the same individual, then the total length of the radius is estimated at 235 mm. The shaft is smaller than that of *Placerias*, while the ends are more laterally expanded but not quite as robust.

Pelvic girdle—An incomplete left ilium, TTU-P11869, is preserved with the acetabulum and parts of the iliac blade missing (Fig. 9A, B). The iliac blade has an anteroposterior length of 221 mm. The ilium possesses two rib facets on its medial face. The posterior rib facet is 21 mm across and the anterior rib facet is 31 mm across at the base and flares out dorsally. The ilium has an anterior blade more similar in profile to *Shansiodon*

TABLE 4. Non-MOTT VPL 3869 (Boren Quarry) dicynodonts also from the Triassic Tecovas Formation (Dockum Group) housed in the TTU collections.

Locality	Specimen/Element
MOTT VPL 0690	TTU-P10492 maxilla fragment; TTU-P10493 jugal-maxilla fragment; TTU-P11447 sternum; TTU-P14283 squamosal; TTU-P15875 maxilla fragment; TTU-P22441 tusk
MOTT VPL 3610	TTU-P22645 squamosal
MOTT VPL 3624	TTU-P09417 left femur
MOTT VPL 3867	TTU-P19224 partial humerus; TTU-P10404 right scapula
MOTT VPL 3873	TTU-P22439 proximal scapula
MOTT VPL 3881	TTU-P10421 left humerus
MOTT VPL 3939	TTU-P18299 vertebrae

than to *Eubrachiosaurus* or *Placerias* (Kammerer et al., 2013:fig. 7). Just dorsal to the acetabulum, the isthmus is also quite narrow, unlike the stahleckeriids *Placerias* and *Eubrachiosaurus* but more similar to *Shansiodon* and *Kannemeyeria* (Kammerer et al., 2013:figs. 7, 8). A partial left pubis, TTU-P18108, is attributed to the new taxon (Fig. 9C). It is a compact element, but dorsoventrally tall with a prominent ventral 'twist' toward the pubic tubercle similar to *Placerias* and *Pentasaurus* (Kammerer, 2018: fig. 11).

DISCUSSION

Phylogenetic Results

For the full dicynodont dataset, a New Technology search with 1000 initial addition sequence replicates found 10 trees having the shortest tree length of 1253.221 (consistency index, 0.245; retention index, 0.752). The consensus of these trees (Fig. 10) differs slightly from recently published iterations of the dataset, such as that of Szczygielski and Sulej (2023), chiefly in the degree of resolution within Kannemeyeriiformes and its subclades. For example, although the Triassic Kannemeyeriiformes are shown to be monophyletic and their interrelationships broadly reflect the results of Szczygielski and Sulej (2023), support is low for some traditional clusters advocated originally by Maisch (2001). The Shansiodontidae of Cox (1965) is shown to be paraphyletic, whereas Stahleckeriidae of Lehman (1961) and Kannemeyeriidae of von Huene (sensu Maisch, 2001) form monophyletic groups. The position of the volatile *Dinodontosaurus*, which sometimes falls just outside *Angonisaurus* + other stahleckeriids (Kammerer et al., 2019) or outside Kannemeyeriidae + Stahleckeriidae (Szczygielski & Sulej, 2023), is unresolved in the present analysis. Within Stahleckeriidae, *Angonisaurus* (Cox & Li, 1983), *Woznikella* (Szczygielski & Sulej, 2023) and several taxa traditionally regarded as 'Stahleckeriinae' form an unresolved polytomy, with a monophyletic Placeriinae nested within this group. Our new taxon, *Argodicynodon*, nests within the Placeriinae subfamily, but its position is poorly resolved within this species-rich clade, a likely consequence of poor character sampling within the group and woefully incomplete fossils. *Zambiasaurus submersus* from the Middle Triassic (Anisian?) of Zambia (Cox, 1969) represents a relatively basally branching placeriine. However, the remaining Late Triassic placeriines all form a polytomy, including *Placerias hesternus*, *Moghreberia nmachouensis*, *Pentasaurus goggai*, *Lisowicia bojani*, and *Argodicynodon boreni*.

Unfortunately, several kannemeyeriiform taxa are based on incomplete specimens with poor character sampling in the current data matrix. Within Placeriinae, for example, prior inclusion of *Pentasaurus* (0% continuous characters coded; 13% numeric characters coded) and *Lisowicia* (30% continuous characters coded; 34% numeric characters coded) produced poor resolution with a polytomy formed by most placeriine taxa (Fig. 10). In a second analysis, we omitted such incomplete taxa to assess the position of *Argodicynodon* relative to the well-represented Late Triassic northern hemisphere placeriines *Moghreberia* and *Placerias*. Other kannemeyeriiform taxa scored for fewer than 50% of characters were excluded. Non-kannemeyeriiform taxa and uninformative characters with respect to Kannemeyeriiformes were also largely excluded to reduce analytical time, but the well-represented *Aulacephalodon bainii*, *Dicynodon angielczyki*, *Lystrosaurus declivis*, and *Lystrosaurus murrayi* were retained for outgroup comparisons. The revised matrix consisted of 29 taxa and 110 characters (23 continuous and 87 numeric), and was analyzed in TNT 1.5 following the same protocol described for the above analysis. The consensus of two most parsimonious trees (Fig. 11) had a length of 326.521 (consistency index, 0.395; retention index, 0.593).

Focusing on the best-sampled kannemeyeriiforms, the revised analysis produced better resolution within the Stahleckeriidae. For example, *Angonisaurus* was shown to be a basal stahleckeriid, and some traditional stahleckeriines formed a monophyletic group (*Sangusaurus*, *Jachaleria*, *Ischigualastia*). Also within Stahleckeriidae, the three best-sampled placeriines—*Argodicynodon*, *Moghreberia*, and *Placerias*—formed a monophyletic clade, albeit with no resolution below the level of the subfamily. Characters shared by Placeriinae at the subfamilial level included: caniniform process long and offset from rest of the snout (char. 15:0→2); maxillary canine present as tusk (interpreted as reversal after loss; char. 22:1→2); temporal portion of skull roof angled dorsally with a strong break in slope (convergent in *Ischigualastia* and Kannemeyeriidae; char. 44:0→1); squamosal dorsoventrally expanded posterior to postorbital bar (char. 62:0→1); circular central depression on occipital condyle between exoccipitals and basioccipital absent (char. 111:0→1); curved ridge between anterior and lateral faces of dentary absent (interpreted as reversal; char. 122:1→0); and triceps tubercle on posterior surface of scapula prominent and 'mound-like' (char. 146:0→1).

Differences with *Placerias* and Other Placeriines

Though rare, enigmatic dicynodont specimens have been reported previously from the Dockum Group in west Texas (Martz et al., 2013). Although *Placerias* and *Argodicynodon* fossils come from different basins, their broad equivalency in age and geography (southwestern U.S.A.) demands a comparison of the new material to the best known and most completely represented North American dicynodont—*Placerias hesternus*—and we suggest several morphological features that help to distinguish these closely related taxa, as well as to distinguish them from other placeriines.

On the snout of *Argodicynodon*, the sutural surface for the premaxilla borders on the maxillary canine alveolus (Fig. 12A). By contrast, in both small and large *Placerias* morphs the maxilla-premaxilla suture is anterodorsally distant from the alveolus, separated by a substantial precaniniform lamina of the maxilla (Fig. 12B). The medial surface of this lamina may bear a small pit ventrally in *Placerias* (Camp & Welles, 1956; Pinto et al., 2022). It is not clear whether the condition shown by *Argodicynodon* or by *Placerias* represents the primitive state because most other nominal placeriines lack well-preserved cranial remains, especially in the snout region. Though well-represented by cranial remains, the sutures in this part of the skull of *Moghreberia*, and therefore the placements of the maxilla-premaxilla suture, are also difficult to interpret (Dutuit, 1980; Olivier, 2020).

The relations of the circumorbital and skull roofing bones differ notably between *Argodicynodon* and *Placerias*. In *Argodicynodon*, the frontal borders the orbit only via a narrow process on the posteriormost corner of the orbital rim, narrowly separating the prefrontal and postorbital (shared in some shansiodontids, kannemeyeriids, and stahleckeriines, and therefore likely representing the primitive condition). In other placeriines that preserve this part of the skull, the prefrontal and postorbital are widely separated, and the frontal contribution to the orbital rim is greater (Kammerer & Ordoñez, 2021:character 40). Despite the smaller overall size of *Argodicynodon*, the pineal foramen is proportionately small, narrow, and teardrop-shaped with a long anteroposterior axis, whereas that of *Placerias* and *Moghreberia* is large and circular. The arrangement of bones surrounding the pineal foramen in *Argodicynodon* is more similar to *Pentasaurus* (Kammerer, 2018:fig. 9) than to *Placerias*, with long posterior processes of the frontal flanking the lateral sides and extending behind the foramen. Like *Pentasaurus* and *Moghreberia*, but unlike *Placerias*, the preparietal is also depressed between the postorbitals rather than "flush" with the rest of the skull roof (character 45). In *Placerias*, the dorsal surface of
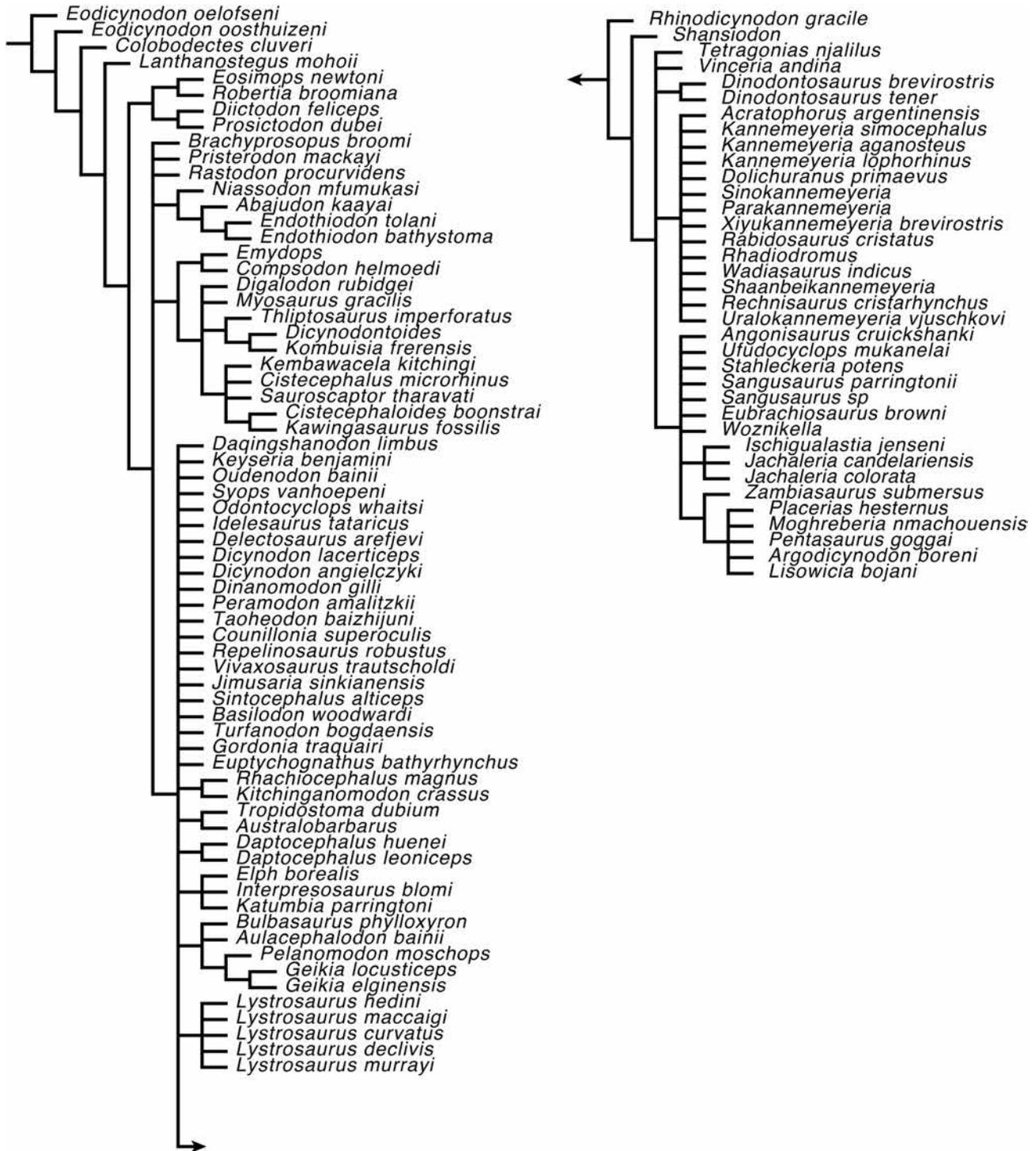
FIGURE 10. Cladogram depicting the interrelationships of Permian through Triassic Dicynodontia, based on the complete dataset of Szczygielski and Sulej (2023) with the addition of *Argodicynodon*. Tree topology represents a reduced strict consensus of 10 most parsimonious trees recovered by a New Technology search with 1000 replicates conducted in TNT 1.5 (Goloboff & Catalano, 2016): tree score, 1253.221; consistency index, 0.245; retention index, 0.752. Non-dicynodont therapsid taxa are not shown due to space limitations; the complete consensus tree with outgroups is provided in the Electronic Supplementary Material.

the preparietal is elevated with the neighboring frontal and parietal bones and is massive with well circumscribed circular borders.

The dentary table of *Argodicynodon*, though shorter than that of *Placerias*, bounds a proportionally narrower and deep median groove bounded by lingual ridges that are parallel-sided throughout their length (Fig. 13A). A narrow, deep groove with parallel sides is also present in *Woznikella*, although the mandible is distinctly medially compressed in this taxon and in *Moghreberia* compared with most others (Szczygielski & Sulej, 2023:fig. 4).
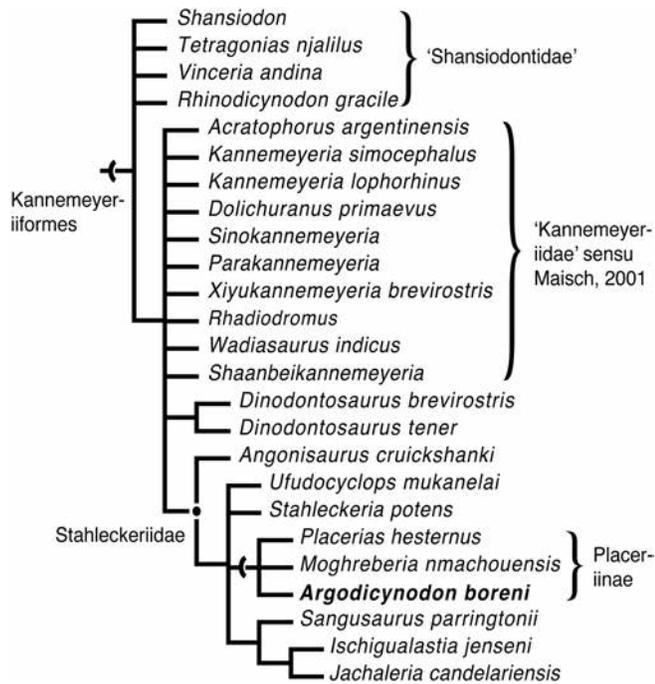
FIGURE 11. Cladogram depicting the interrelationships of Triassic Kannemeyeriiformes, based on the pruned dataset of Szczygielski and Sulej (2023) excluding non-kannemeyeriiform taxa and uninformative characters, and including only taxa with more than 50% of characters coded for completeness. Tree topology represents a reduced strict consensus of two most parsimonious trees recovered by a New Technology search with 1000 replicates conducted in TNT 1.5 (Goloboff & Catalano, 2016): tree score, 326.521; consistency index, 0.395; retention index, 0.593. The complete consensus tree is provided in the Supplementary Files.

In *Placerias*, the median groove is restricted posteriorly where the lingual ridges bulge toward the midline, then opens anteriorly into a shallow bowl (Fig. 13B).

The articular of *Argodicynodon* is autapomorphic in having a tab-like medial process that is greatly expanded into a "tongue-like" shelf. The proportions of this tab-like process are medio-laterally wider than the main saddle-shaped fossa for the quadrate (Fig. 13C). In *Placerias*, this tab-like extension is only modest and is medio-laterally narrower than the quadrate roller (Fig. 13D).

The scapulocoracoid of *Argodicynodon* is very gracile compared with that of *Placerias*, but bears striking similarity to that of *Woznikella* (Szczygielski & Sulej, 2023:fig. 11). Whereas the scapular blade of *Placerias* is broad and parallel-sided on its anterior and posterior edges, across a range of small and large specimens, that of *Woznikella* and *Argodicynodon* tapers near the acromion to form a narrow "neck" region (Fig. 8A). In summary, the combination of derived *Placerias*-like features and primitive *Woznikella*- and *Pentasaurus*-like morphology strongly suggests an intermediate position for *Argodicynodon* in placeriine phylogeny, but more fossils are needed to further evaluate these relationships.

Boren Quarry and its Associated Synapsid Fauna

A complete list of taxa from the Boren Quarry is provided in Table 3. Along with the dicynodont synapsid *Argodicynodon*, Mueller (2016) reported isolated teeth of a possible *Ecteninion*-like cynodont from the Boren Quarry. The identification of these teeth was based on their sectorial shape with serrations

and lacking a cingulum, a combination that is unique to ecteniniids among cynodonts. However, these features are also primitive in theriodont synapsids and archosaurs, and the coarse cusp arrangements do not resemble those of other Triassic cynodonts—i.e., the corresponding homologous 'a,' 'b,' and 'c' cusps are not clearly defined (AKH, pers. obs.). The teeth also lack preserved roots and resemble shed archosaur teeth in this respect. So, it remains equally plausible that the Dockum teeth represent an as yet unknown archosaur. At present, ecteniniids are known exclusively from older Ladinian-Carnian-aged rocks in Brazil and Argentina (Martinelli et al., 2017), and the putative Boren cynodont records are thus excluded from the faunal list in Table 3. This leaves *Argodicynodon* as the only definitive synapsid taxon from the Boren Quarry to date.

Taxic Diversity of Triassic Dicynodonts from Western North America

To date, *Placerias* and *Eubrachiosaurus*—both stahleckeriids—have represented the only valid named dicynodonts from the Triassic of North America, although additional materials have been reported from the Middle Triassic Moenkopi Formation in Arizona (Nesbitt & Angielczyk, 2002) and Economy Member of the Wolfville Formation in Nova Scotia (Sues et al., 2022), Upper Triassic Evangeline Member of the Wolfville Formation (Baird & Olsen, 1983; Sues & Olsen, 2015; Sues et al., 2022), and Upper Triassic Pekin Formation in North Carolina (Green et al., 2005; Green, 2012) (Table 1). *Argodicynodon boreni* preserves a number of cranial and postcranial characters that support that it is a new kannemeyeriiform similar to but distinct from *Placerias* and *Eubrachiosaurus*. Our new placeriine record and other dicynodont material from the Dockum Group (Tables 1, 4; Fig. 14) support a more diverse North American Triassic dicynodont fauna than previously known. Moreover, with recent chronostratigraphic age constraints for the *Placerias* Quarry, the *Argodicynodon* beds within the Boren Quarry are approximately seven million years older than the *Placerias* Quarry beds, with some of the other Dockum dicynodont material presumed to be even older (Ramezani et al., 2014).

The Museum of Texas Tech now has in its collection over 36 dicynodont elements from eight Dockum Group sites, including the Boren Quarry (Tables 2, 4). The collection represents a minimum of 14 individuals from these eight sites (Mueller, 2016). Of the possible dicynodont elements collected from Dockum sites other than the Boren Quarry three are relatively complete and readily identifiable as kannemeyeriiforms (Fig. 14), while the rest are fragmentary and are only provisionally listed as dicynodonts. A scapula, TTU-P10404 (Fig. 14A), was collected from the locality MOTT VPL 3867 14 km to the north and stratigraphically lower than the Boren Quarry (Martz, 2008). The scapula is not referred to *Argodicynodon* because of its morphological differences with the scapulae collected at the Boren Quarry. A humerus, TTU-P10421 (Fig. 14B), was collected from MOTT VPL 3881, 6 km to the west-southwest and stratigraphically higher than the Boren Quarry. A femur, TTU-P09417 (Fig. 14C), was collected from MOTT VPL 3624 18 km to the northwest, from just below the Trujillo Formation (figured in Martz et al., 2013:fig. 16). The femur cannot be compared with *Argodicynodon* because the femur of *Argodicynodon* is unknown, and thus the material remains indeterminate beyond Kannemeyeriiformes at present. It is possible all three elements could represent other new species or dimorphism. Regardless of a more precise identification of the non-Boren material, this material indicates that dicynodonts were more common in the southern Dockum deposits of west Texas than previously known. A life reconstruction of *Argodicynodon* is shown in Figure 15.
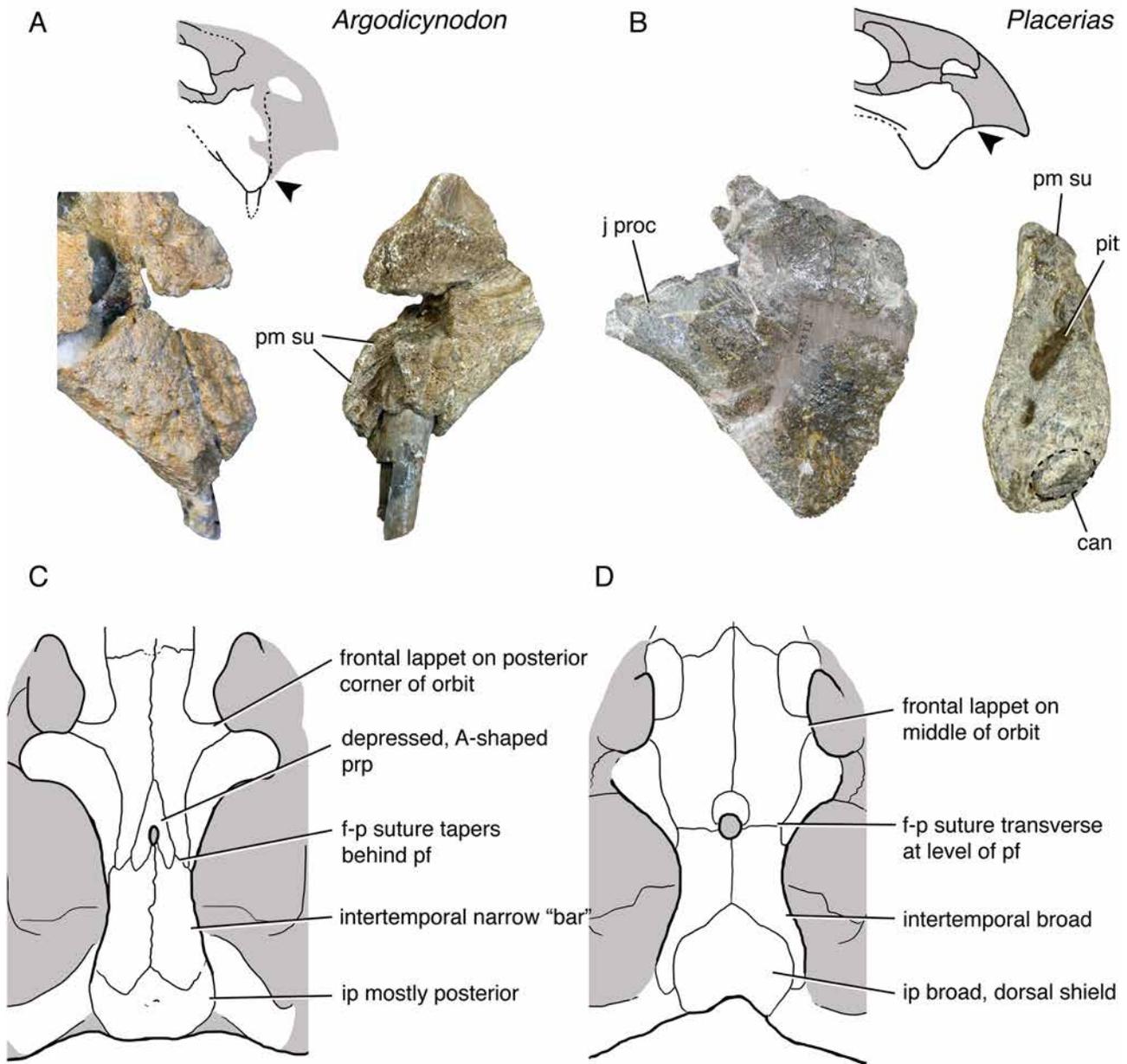
FIGURE 12. Comparisons between *Argodicynodon* (**A**, **C**) and *Placerias* (**B**, **D**). **A**, maxillary morphology in *Argodicynodon* (TTU-P10402) preserves the location of the premaxilla-maxilla suture (serrate surface shown as '**pm su**'), shown in right lateral (left) and anteromedial (right) views. **B**, same region of right maxilla in a 'small morph' specimen of *Placerias* (UCMP 27552) showing the anterior 'pit.' Arrowheads indicate position of premaxilla-maxilla suture: ventrally on the canine alveolus in **A**; anterodorsally far from the alveolus (above a unique anterior pit) in **B**. **C**, reconstruction of dorsal skull roof of *Argodicynodon* based on TTU-P10402 and TTU-P18107. **D**, reconstruction of dorsal skull roof of *Placerias* based on Cox (1965). **A**–**D** are not shown to scale. **Abbreviations**: **can**, canine alveolus; **f-p**, frontoparietal; **ip**, interparietal; **j proc**, jugal process of maxilla; **pf**, pineal (parietal) foramen; **pm su**, suture for premaxilla; **prp**, preparietal.

Argodicynodon and Dicynodont Biogeography during the Late Triassic

For decades, South American Late Triassic dicynodonts represented the richest dicynodont records in the Upper Triassic and certainly in the western hemisphere (Kammerer & Ordoñez, 2021), and their diversity and temporal distributions provide a basis for Upper Triassic South American biostratigraphy. Middle-to-Early Late Triassic (Ladinian–Carnian) dicynodont assemblages in South America included the kannemeyeriid *Acratophorus*, non-kannemeyeriid

kannemeyeriiforms *Dinodontosaurus* (two species), and the stahleckeriids *Stahleckeria* and *Ishigualastia* (Kammerer & Ordoñez, 2021). Dicynodont numbers and diversity clearly waned in South America by Norian times, with identifiable Norian taxa attributed to Stahleckeriidae (e.g., *Jachaleria*) (Kammerer & Ordoñez, 2021; Martinelli et al., 2021). In Africa, dicynodont fossils become very rare within the Upper Triassic, with only the Norian placeriine *Pentasaurus* represented (Kammerer, 2018). To date, the Middle Triassic *Zambiasaurus* and the Late Triassic *Pentasaurus* are the only placeriines documented in
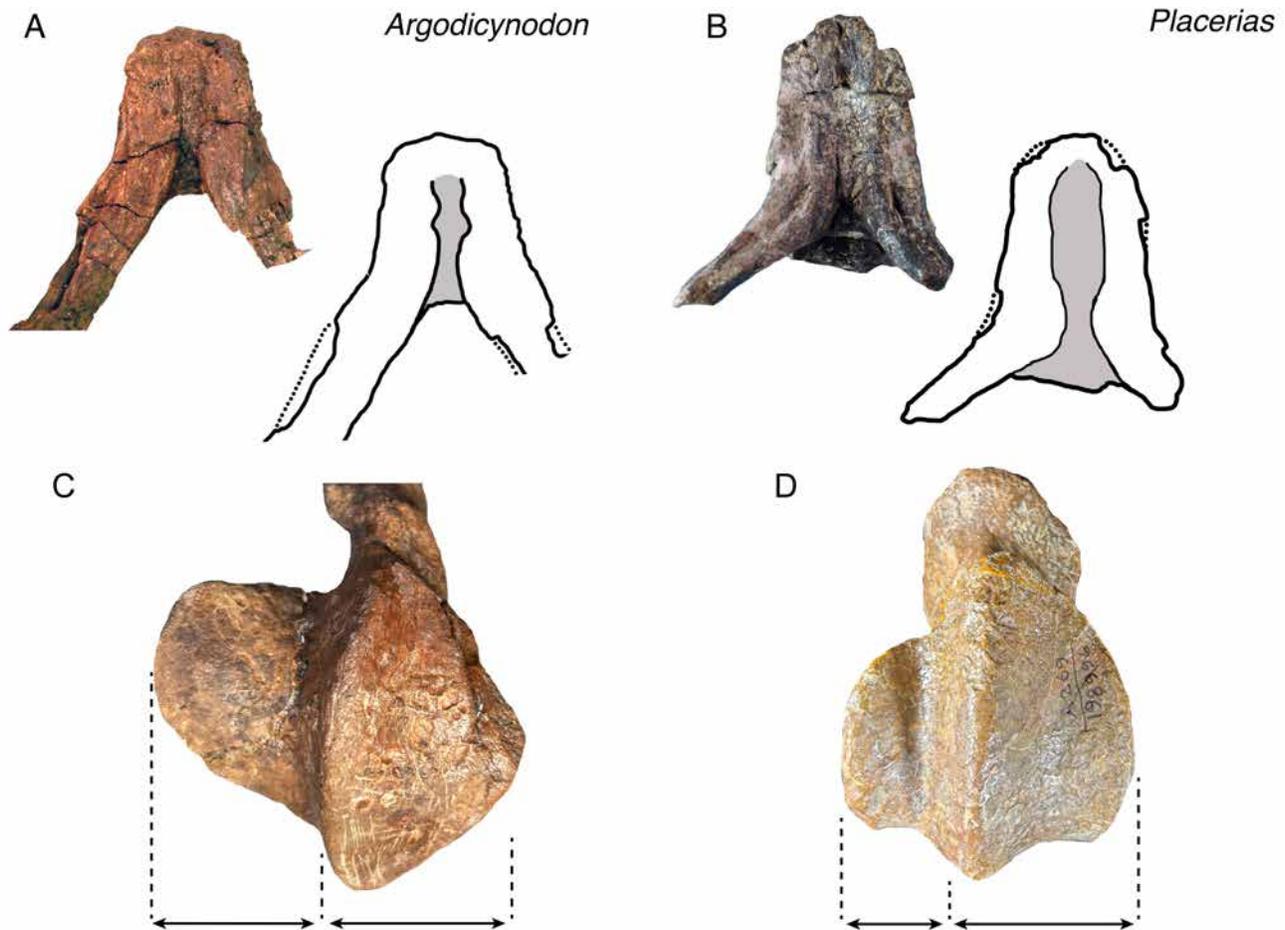
FIGURE 13. Comparisons between *Argodicynodon* and *Placerias* (continued). **A**, anterior portion of mandible of *Argodicynodon*, TTU-P09421, in dorsal view. **B**, anterior mandible of *Placerias*, UCMP 24740, in dorsal view. **C**, right articular of *Argodicynodon*, TTU-P09421, viewed in dorsal aspect (anterior direction toward top of page). **D**, right articular of *Placerias*, UCMP 198996, viewed in dorsal aspect. Note the enlarged tab-like medial process in **C** which bears a broader transverse width than the lateral articular surface for the quadrate condyle. Specimens are not shown to scale.

southern Pangea, but they suggest a reasonably widespread geographic range for Placeriinae by Norian times albeit in the form of different species in different basins.

In Laurasia, stahleckeriid records are also rare during the Upper Triassic with Carnian occurrences in Germany (Schoch, 2012), Poland (Sczygielski & Sulej, 2021), and in North America the Newark Supergroup (Baird & Patterson, 1968; Green et al., 2005; Huber et al., 1993). There are isolated Norian occurrences in the Chinle and Popo Agie formations (Kammerer et al., 2013), and the more densely concentrated occurrences of *Placerias* in the Chinle Formation *Placerias* Quarry (Camp & Welles, 1956), and in central Europe the enormous placeriine *Lisowicia* (Dzik et al., 2008: Sulej & Niedźwiedski 2019) and *Woznikella* (Szczygielski & Sulej, 2023). This makes *Argodicynodon* a rare western occurrence of a non-*Placerias* placeriine in an otherwise depauperate Norian dicynodont assemblage. Elsewhere in the northern hemisphere, in Germany and Poland, dicynodonts spanned from the Carnian (Schoch, 2012; Sczygielski & Sulej, 2021) through the Norian and Rhaetian, respectively (Dzik et al., 2008; Sulej & Niedźwiedzki, 2019). These records, however, belong to kannemeyeriiforms of unknown affinity (as in the German record) or to other placeriine stahleckeriids (as in the Polish records). As discussed above,

future collecting in undersampled basins has the potential to broaden our understanding of the biogeographic histories of kannemeyeriiforms from Middle to Late Triassic times and their ultimate disappearance from the terminal Triassic Laurasian fauna.

CONCLUSIONS

Here, we have described a new dicynodont from the Upper Triassic Tecovas Formation (Dockum Group) based on numerous specimens collected from the Boren Quarry in Garza County, Texas. The specimens provide the basis of a new genus and species, *Argodicynodon boreni*, which is shown conservatively to be a member of the Placeriinae and is anatomically distinct from the better-known northern hemisphere placeriines *Placerias* and *Moghreberia*. This is the first nominal kannemeyeriiform from Texas and represents an early datum (early Norian) for a placeriine stahleckeriid as the group became established in western North America. This discovery, along with other dicynodont material from other Dockum Group localities in west Texas, adds to the Late Triassic dicynodont record of Laurasia and, along with the recent records from Poland and Germany, broadens our understanding of northern hemisphere dicynodont diversity during this time.
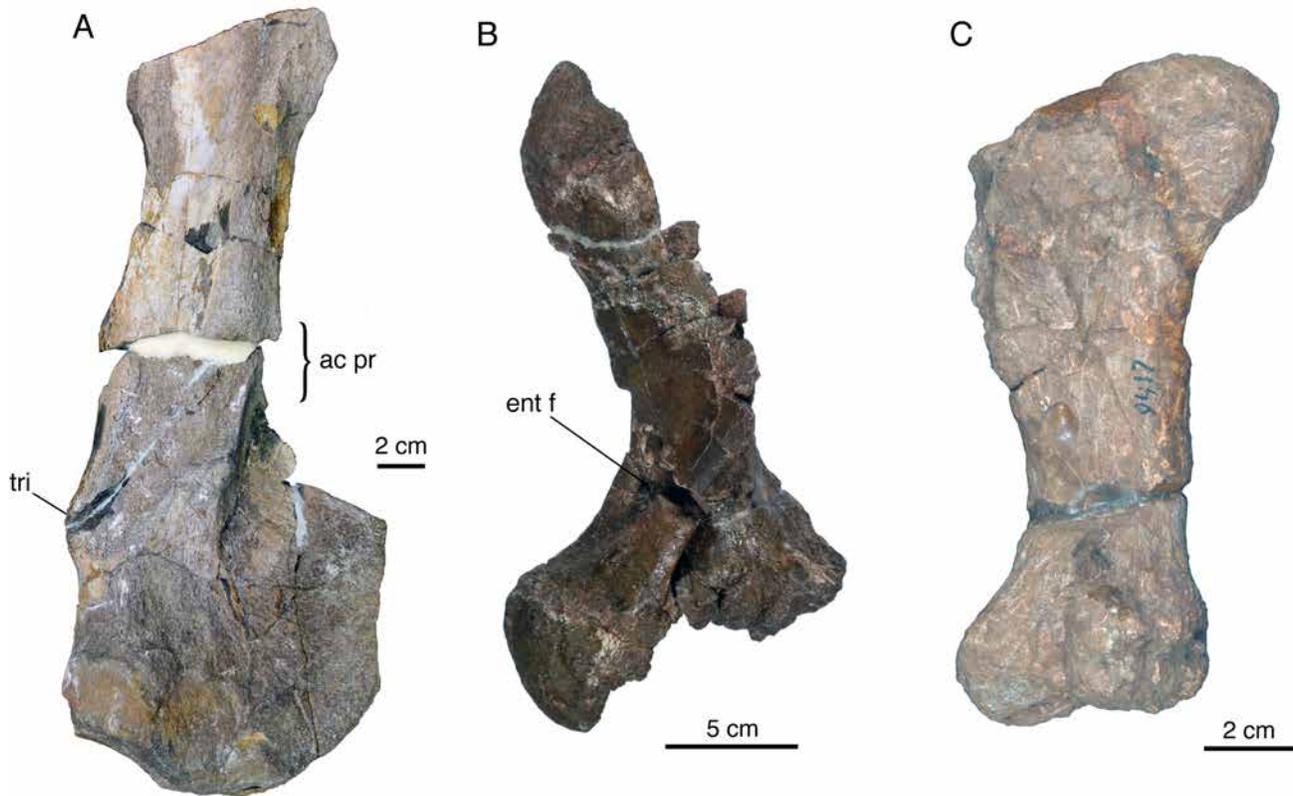
FIGURE 14. A selected representation of other (Non-MOTT VPL 3869) dicynodont material from the Triassic Dockum Group housed in the TTU collections. **A**, right partial scapula, TTU-P10404 in lateral view (anterior to right); **B**, left humerus, TTU-P10421 in ventral view; **C**, left femur from the Post Quarry (MOTT VPL 3624), TTU-P09417 in ventral view. A catalog of non-Boren dicynodonts housed in the TTU collections and their provenance is listed in Table 4. **Abbreviations**: **ac pr**, broken area for acromion process; **ent f**, entepicondylar foramen; **tri**, triceps tubercle.

FIGURE 15. Life reconstruction of *Argodicynodon boreni*.

DISCLOSURE STATEMENT

No potential conflict of interest was reported by the author(s).

AUTHOR CONTRIBUTIONS

BDM designed the project and wrote sections for the initial draft as part of his unpublished doctoral dissertation. AKH and BJS collected data, revised and edited the manuscript, drafted and revised the figures, and performed the phylogenetic analyses. AKH and JLP collected additional comparative data and photographs from *Placerias*. KD-W and SC provided

additional data and photographs. All authors edited the manuscript.

SUPPLEMENTARY FILES

Supplementary Data 1: Detailed methods (supplementary Appendices S1–S5).

Supplementary Data 2: NEXUS-formatted file for cladistic analysis (complete dataset).

Supplementary Data 3: NEXUS-formatted file for cladistic analysis (pruned kannemeyeriiform dataset).

Supplementary Data 4: TNT-formatted file of complete analysis.

Supplementary Data 5: TNT-formatted file of reduced analysis.

ORCID

Adam K. Huttenlocker http://orcid.org/0000-0002-7335-3208

LITERATURE CITED

Abdala, F., C. A. Marsicano, R. M. H. Smith, & R. Swart. (2013). Strengthening western Gondwanan correlations: a Brazilian dicynodont (Synapsida, Anomodontia) in the Middle Triassic of Namibia. *Gondwana Research 23*, 1151–1162.

Angielczyk K. D. (2001). Preliminary phylogenetic analysis and stratigraphic congruence of the dicynodont anomodonts (Synapsida: Therapsida). *Palaeontologica Africana*, *37*, 53–79.

Angielczyk, K. D., & A. A. Kurkin. (2003). Phylogenetic Analysis of Russian Permian dicynodonts (Therapsida: Anomodontia): implications for Permian biostratigraphy and Pangaean biogeography. *Zoological Journal of the Linnean Society*, *139*, 157–212.

Angielczyk, K. D., Steyer, J. S., Sidor, C. A., Smith, R. M., Whatley, R. L., & Tolan, S. (2014a). Permian and Triassic dicynodont (Therapsida: Anomodontia) faunas of the Luangwa Basin, Zambia: taxonomic update and implications for dicynodont biogeography and biostratigraphy. In C. F. Kammerer, K. D. Angielczyk, & J. Fröbisch (Eds.), *Early Evolutionary History of the Synapsida* (pp. 93–138). Springer.

Angielczyk, K. D., Huertas, S., Smith, R. M., Tabor, N. J., Sidor, C. A., Steyer, J. S., … & Gostling, N. J. (2014b). New dicynodonts (Therapsida, Anomodontia) and updated tetrapod stratigraphy of the Permian Ruhuhu Formation (Songea Group, Ruhuhu Basin) of southern Tanzania. *Journal of Vertebrate Paleontology*, *34*(6), 1408–1426.

Angielczyk, K. D., Hancox, P. J., & Nabavizadeh, A. (2017). A redescription of the Triassic kannemeyeriiform dicynodont *Sangusaurus* (Therapsida, Anomodontia), with an analysis of its feeding system. *Journal of Vertebrate Paleontology*, *37*(sup1), 189–227.

Baird, D., & O. F. Patterson III. (1968). Dicynodont-archosaur fauna in the Pekin Formation (Upper Triassic) of North Carolina. *Geological Society of America Special Paper*, *115*, 11.

Baird, D., & P. E. Olsen. (1983). Late Triassic herpetofauna from the Wolfville Formation of the Minas Basin (Fundy Basin), Nova Scotia, Canada. *Geological Society of America, Abstracts with Programs*, *15*(3), 122.

Bandyopadhyay, S. (1988). A kannemeyeriid dicynodont from the Middle Triassic Yerrapalli Formation. *Philosophical Transactions of the Royal Society of London B Biological Sciences*, *320*, 185–233.

Battail, 1993. B. (1993). On the biostratigraphy of the Triassic therapsid-bearing formations. *New Mexico Museum of Natural History and Science Bulletin*, *3*, 31–35.

Bonaparte, J. F. (1966). Una nueva fauna "triásica" de Argentina (Therapsida: cynodontia Dicynodontia): consideraciones filogenéticas y paleobiogeográficas. *Ameghiniana*, *4*, 243–296.

Broom, R. (1905). On the use of the term Anomodontia. *Records of the Albany Museum*, *1*, 266–269.

Camp, C. L. (1956). Triassic dicynodont reptiles, Part II: Triassic dicynodonts compared. *Memoirs of the University of California*, *13*, 305–341.

Camp, C. L., & S. P. Welles. (1956). Triassic dicynodont reptiles, Part I: The North American genus *Placerias*. *Memoirs of the University of California*, *13*, 255–304.

Case, E. C. (1922). New reptiles and stegocephalians from the Upper Triassic of western Texas. *Carnegie Institute of Washington Publication*, *321*, 1–84.

Cather, S. M., K. E. Zeigler, G. H. Mack, and S. A. Kelley. (2013). Toward standardization of Phanerozoic stratigraphic nomenclature in New Mexico. *Rocky Mountain Geology*, *48*, 101–124.

Cox, C. B. (1959). On the anatomy of a new dicynodont genus with evidence of the position of the tympanum. *Proceedings of the Zoological Society of London*, *132*, 321–367.

Cox, C. B. (1965). New Triassic dicynodonts from South America, their origins and relationships. *Philosophical Transactions of the Royal Society of London B*, *248*, 457–514.

Cox, C. B. (1969). Two new dicynodonts from the Triassic Ntawere Formation, Zambia. *Bulletin of the British Museum (Natural History), Geology*, *17*, 257–294.

Cox, C. B. (1991). The Pangaea dicynodont *Rechnisaurus* and the comparative biostratigraphy of Triassic dicynodont faunas. *Palaeontology*, *34*, 767–784.

Cox, C. B. (1998). The jaw function and adaptive radiation of the dicynodont mammal-like reptiles of the Karoo basin of South Africa. *Zoological Journal of the Linnean Society*, *122*, 349–384.

Cox, C. B., & J.-L. Li. (1983). A new genus of Triassic dicynodont from East Africa and its classification. *Palaeontology*, *26*, 389–406.

Damiani, R., C. Vasconcelos, A. Renaut, J. Hancox, & A. Yates. (2007). *Dolichuranus primaevus* (Therapsida: Anomodontia) from the Middle Triassic of Namibia and its phylogenetic relationships. *Palaeontology*, *50*, 1531–1546.

Dutuit, J.-M. (1980). Principaux caractères d'un genre de Dicynodonte du Trias marocain. *C. R. Acad. Sc. Paris*, *290*, 655–658.

Dzik, J., T. Sulej, & G. Niedźwiedzki. (2008). A dicynodont-theropod association in the latest Triassic of Poland. *Acta Palaeontologica Polonica*, *53*, 733–738.

Goloboff, P. A., & S. A. Catalano. (2016). TNT version 1.5, including a full implementation of phylogenetic morphometrics. *Cladistics*, *32*, 221–238. https://doi.org/10.1111/cla.12160

Goloboff, P. A., C. I. Mattoni, & A. S. Quinteros. (2006). Continuous characters analyzed as such. *Cladistics*, *22*, 589–601.

Green, J., V. Schneider, M. Schweitzer, & J. Clarke. (2005). New evidence for non-*Placerias* dicynodonts in the Late Triassic (Carnian-Norian) of North America. *Journal of Vertebrate Paleontology*, *25* (3, Supplement), 65A–66A.

Green, J. L. (2009). *Enamel-Reduction and Orthodentine in Dicynodontia (Therapsida) and Xenarthra (Mammalia): An Evaluation of the Potential Ecological Signal Revealed by Dental Microwear* [Unpublished doctoral dissertation]. North Carolina State University, Raleigh.

Green, J. L. (2012). Bone and dental histology of Late Triassic dicynodonts from North America. In A. Chinsamy-Turan (Ed.), *Forerunners of Mammals: Radiation, Histology, Biology* (pp. 178–196). Indiana University Press, Bloomington.

Groenewald, G. H., & J. W. Kitching. (1995). Biostratigraphy of the *Lystrosaurus* Assemblage Zone. In B. S. Rubidge (Ed.), *Biostratigraphy of the Beaufort Group (Karoo Supergroup)* (pp. 35–39). South African Committee for Stratigraphy, Biostratigraphic Series 1.

Hancox, J. P., K. D. Angielczyk, & B. S. Rubidge. (2013). *Angonisaurus* and *Shansiodon*, dicynodonts (Therapsida, Anomodontia) from subzone C of the *Cynognathus* assemblage zone (Middle Triassic) of South Africa. *Journal of Vertebrate Paleontology*, *33*, 655–676.

Hopson, J. A. (1984). Late Triassic traversodont cynodonts from Nova Scotia and southern Africa. *Palaeontologia Africana*, *25*, 181–201.

Huber, P., S. G. Lucas, & A. P. Hunt. (1993). Revised age and correlation of the Upper Triassic Chatham Group (Deep River Basin, Newark Supergroup), North Carolina. *Southeastern Geology*, *33*, 171–193.

Huene, F. von. (1935). *Die fossilien Reptilien des südamerikanischen Gondwanalandes an der Zeitenwend*. Lieferung I. Heine, Tübingen, 1–92.

Huene, F. von. (1948). Short review of the lower tetrapods. In A. Du Toit (Ed.), *Robert Broom Commemorative Volume, Spec. Publ. Roy. Soc. S. Afr., Cape Town* (pp. 65–106). Royal Society of South Africa, Cape Town.

Hunt A. P., V. L. Santucci, M. G. Lockley, & T. J. Olson. (1993). Dicynodont trackways from the Holbrook Member of the Moenkopi Formation (Middle Triassic: Early Anisian), of

Arizona. In S. G. Lucas & M. Morales (Eds.), *The Nonmarine Triassic: New Mexico Museum of Natural History and Science Bulletin 3* (pp. 213–218). New Mexico Museum of Natural History and Science.

Kammerer, C. F. (2018). The first skeletal evidence of a dicynodont from the lower Elliot Formation of South Africa. *Palaeontologica Africana*, *52*, 102–128.

Kammerer, C. F., J. Fröbisch, & K. D. Angielczyk. (2013). On the validity and phylogenetic position of *Eubrachiosaurus browni*, a kanne-meyeriiform dicynodont (Anomodontia) from the Triassic of North America. *PLoS ONE*, *8*, e64203. https://doi:10.1371journal.pone.0064203

Kammerer, C. F., P. A. Viglietti, P. J. Hancox, R. J. Butler, & J. N. Choiniere. (2019). A new kannemeyeriiform dicynodont (*Ufudocyclops mukanelai*, gen. et sp. nov.) from subzone C of the *Cynognathus* Assemblage Zone, Triassic of South Africa, with implications for biostratigraphic correlation with other African Triassic faunas. *Journal of Vertebrate Paleontology*, *39*, e1596921. https://doi.org/10.1080/02724634.2019.1596921

Kammerer, C. F., & M. de los A. Ordóñez. (2021). Dicynodonts (Therapsida: Anomodontia) of South America. *Journal of South American Earth Sciences*, *108*, 103171.

King, G. M. (1988). Anomodontia. In P. Wellnhofer (Ed.), *Handbuch der Paläoherpetologie, 17 C* (pp. 1–174). Gustav Fischer Verlag, Stuttgart.

King, G. M. (1993). Species longevity and generic diversity in dicynodont mammal-like reptiles. *Palaeogeography, Palaeoclimatology, Palaeoecology*, *102*(3-4), 321–332.

Kitching, J. W. (1995a). Biostratigraphy of the *Dicynodon* assemblage zone. In B. S. Rubidge (Ed.), *Biostratigraphy of the Beaufort Group (Karoo Supergroup)* (pp. 29–34). South African Committee for Stratigraphy, Biostratigraphic Series 1.

Kitching, J. W. (1995b). Biostratigraphy of the *Cynognathus* Assemblage Zone. In B. S. Rubidge (Ed.), *Biostratigraphy of the Beaufort Group (Karoo Supergroup)* (pp. 40–45). South African Committee for Stratigraphy, Biostratigraphic Series 1.

Lehman, J.-P. (1961). Dicynodontia. In J. -P. Piveteau (Ed.), *Traité de Paléontologie, VI, Mammifères, Vol 1: Origine Reptilienne évolution* (pp. 287–351). Masson et Cie, Paris.

Lehman, T. M., & S. Chatterjee. (2005). The depositional setting and vertebrate biostratigraphy of the Triassic Dockum Group of Texas. *Indian Journal of Earth System Science*, *114*, 325–351.

Lehman, T. M., S. Chatterjee, & J. P. Schnable. (1992). The Cooper Canyon Formation (Late Triassic) of western Texas. *Texas Journal of Science*, *44*, 349–355.

Lessner, E. J., W. G. Parker, A. D. Marsh, S. J. Nesbitt, R. B. Irmis, & B. D. Mueller. (2018). New insights into Late Triassic dinosauromorph-bearing assemblages from Texas using apomorphy-based identifications. *PaleoBios*, *35*, 1–41.

Long, R. A., & P. A. Murry. (1995). Late Triassic (Carnian and Norian) tetrapods from the southwestern United States. *New Mexico Museum of Natural History and Science Bulletin*, *4*, 1–254.

Lucas, F. A. (1904). A new batrachian and a new reptile from the Triassic of Arizona. *Proceedings of the United States National Museum*, *27*, 193–195.

Lucas, S. G. (1995). Triassic dicynodont biochronology. *Albertania*, *16*, 33–40.

Lucas, S. G. (1998a). Global Triassic biostratigraphy and biochronology. *Palaeogeography, Palaeoclimatology, Palaeoecology*, *143*, 347–384.

Lucas, S. G. (1998b). *Placerias* (Reptilia, Dicynodontia) from the Upper Triassic of the Newark Supergroup, North Carolina, USA, and its biostratigraphic significance. *Neues Jahrbuch für Geologie und Paläontologie Monatschefte*, *1998*, 432–448.

Lucas, S. G., & A. P. Hunt. (1989). Revised Triassic stratigraphy in the Tucumcari basin, east-central New Mexico. In S.G. Lucas & A.P. Hunt (Eds.), *Dawn of the age of dinosaurs in the American Southwest* (pp. 150–170). New Mexico Museum of Natural History & Science.

Lucas, S. G., & A. P. Hunt. (1993a). A dicynodont from the Upper Triassic of New Mexico and its biochronological significance. *New Mexico Museum of Natural History and Science Bulletin*, *3*, 321–326.

Lucas, S. G., & A. P. Hunt. (1993b). Tetrapod biochronology of the Chinle Group (Upper Triassic), western United States. *New Mexico Museum of Natural History and Science Bulletin*, *3*, 327–329.

Maisch, M. W. (2001). Observations on Karoo and Gondwana vertebrates. Part 2: A new skull reconstruction of *Stahleckeria potens* von Huene, 1935 (Dicynodontia, Middle Triassic) and a reconsideration of kannemeriiform phylogeny. *Neues Jahrbuch für Geologie und Paläontologie, Abhandlungen*, *220*, 127–152.

Martinelli, A. G., M. B. Soares, T. V. de Oliveira, P. G. Rodrigues, & C. L. Schultz. (2017). The Triassic eucynodont *Candelariodon barberenai* revisited and the early diversity of stem prozostrodontians. *Acta Palaeontologica Polonica*, *62*, 527–542.

Martinelli, A. G., J. A. Escobar, H. Francischini, L. Kerber, R. T. Müller, R. Rubert, C. L. Schultz, & Á. A. S. Da-Rosa. (2021). New records of a stahleckeriid dicynodont (Therapsida, Dicynodontia) from the Late Triassic of southern Brazil and biostratigraphic remarks on the *Riograndia* Assemblage Zone. *Historical Biology*, *33*(11), 3101–3110. http://doi.org/10.1080/08912963.2020.1850715

Martz, J. W. (2008). *Lithostratigraphy, chemostratigraphy, and vertebrate biostratigraphy of the Dockum Group (Upper Triassic), of southern Garza County, west Texas* [Unpublished doctoral dissertation]. Texas Tech University, Lubbock, Texas.

Martz, J. W., B. Mueller, S. J. Nesbitt, M. R. Stocker, W. J. Parker, M. Atanassov, N. Fraser, J. Weinbaum, & J. R. Lehane. (2013). A taxonomic and biostratigraphic re-evaluation of the Post Quarry vertebrate assemblage from the Cooper Canyon Formation (Dockum Group, Upper Triassic) of southern Garza County, western Texas. *Earth and Environmental Science Transactions of the Royal Society of Edinburgh*, *103*, 339–364.

Mueller, B. D. (2016). *Triassic tetrapod paleontology and taphonomy of the Boren Quarry, Dockum Group, Garza County, Texas.* [Unpublished doctoral dissertation]. Texas Tech University, Lubbock, Texas.

Mueller, B., & S. Chatterjee. (2007). Dicynodonts (Synapsida: Therapsida) from the Late Triassic Dockum Group of Texas. *Journal of Vertebrate Paleontology*, *27*(3, Supplement), 121A.

Nesbitt, S. J., & K. D. Angielczyk. (2002). New evidence of large dicynodonts in the upper Moenkopi Formation (Middle Triassic) of northern Arizona. *PaleoBios*, *22*, 10–17.

Olivier, C. (2020). *Phylogeny, paleobiogeography, and paleophysiology of the Triassic dicynodonts (Therapsida, Anomodontia): contributions of the Laotian and Moroccan forms.* [Unpublished doctoral dissertation]. Sorbonne Université, Paris.

Olson, E. C. (1944). Origin of mammals based upon the cranial morphology of the therapsid suborders. *Geological Society of America Special Papers*, *55*, 1–136.

Osborn, H. F. (1903). On the primary division of the Reptilia into two sub-classes, Synapsida and Diapsida. *Science*, *17*, 275–276.

Owen, R. (1859). On some reptilian remains from South Africa. *Edinburgh New Philosophical Journal*, *10*, 289–291.

Parker, W. G., & J. W. Martz. (2011). The Late Triassic (Norian) Adamanian-Revueltian tetrapod faunal transition in the Chinle Formation of Petrified Forest National Park, Arizona. *Earth and Environmental Science Transactions of the Royal Society of Edinburgh*, *101*, 231–260.

Pinto, J., D. Varajao de Latorre, C. Marshall, & S. J. Nesbitt. (2022). Evidence for sexual dimorphism, in both size and variance, in *Placerias hesternus* revealed through measurement of the maxillary caniniform process. *Geological Society of America Abstracts with Programs*, *54*(5). https://doi: 10.1130abs/2022AM-381084

Ramezani, J., D. E. Fastovsky, & S. A. Bowring. (2014). Revised chronostratigraphy of the lower Chinle Formation strata in Arizona and New Mexico (USA): High-precision U-Pb geochronological constraints on the Late Triassic evolution of dinosaurs. *American Journal of Science*, *314*, 981–1008.

Rubidge, B. S. (1995). *Biostratigraphy of the Beaufort Group (Karoo Supergroup)*. South African Committee for Stratigraphy Biostratigraphic Series 1.

Rubidge, B. S. (2005). Re-uniting lost continents—fossil reptiles from the ancient Karoo and their wanderlust. *South African Journal of Geology*, *108*, 135–172.

Schoch, R. R. (2012). A dicynodont mandible from the Triassic of Germany forms the first evidence of large herbivores in the Central European Carnian. *Neues Jahrbuch für Geologie und Paläontologie, Abhandlungen*, *263*, 119–123.

Smith, R. M. H., B. S. Rubidge, M. O. Day, & J. Botha. (2020). Introduction to the tetrapod biozonation of the Karoo Supergroup. *South African Journal of Geology*, *123*, 131–140.

Smith, R. M. H., & A. W. Keyser. (1995a). Biostratigraphy of the *Tapinocephalus* assemblage zone. In B. S. Rubidge (Ed.), *Biostratigraphy of the Beaufort Group (Karoo Supergroup)* (pp. 8–12). South African Committee for Stratigraphy, Biostratigraphic Series 1.

Smith, R. M. H., & A. W. Keyser. (1995b). Biostratigraphy of the *Pristerognathus* assemblage zone. In B. S. Rubidge (Ed.), *Biostratigraphy of the Beaufort Group (Karoo Supergroup)* (pp. 13–17). South African Committee for Stratigraphy, Biostratigraphic Series 1.

Smith, R. M. H., & A. W. Keyser. (1995c). Biostratigraphy of the *Tropidostoma* assemblage zone. In B. S. Rubidge (Ed.), *Biostratigraphy of the Beaufort Group (Karoo Supergroup)* (pp. 18–22). South African Committee for Stratigraphy, Biostratigraphic Series 1.

Smith, R. M. H., & A. W. Keyser. (1995d). Biostratigraphy of the *Cistecephalus* assemblage zone. In B. S. Rubidge (Ed.), *Biostratigraphy of the Beaufort Group (Karoo Supergroup)* (pp. 23–28). South African Committee for Stratigraphy, Biostratigraphic Series 1.

Sookias, R. B., R. J. Butler, & R. B. J. Benson. (2012). Rise of dinosaurs reveals major body-size transitions are driven by passive processes of trait evolution. *Proceedings of the Royal Society B*, *279*, 2180–2187.

Stocker, M. R. (2013). A new taxonomic arrangement for *Paleorhinus scurriensis*. *Earth and Environmental Science Proceedings of the Royal Society of Edinburgh*, *103*, 251–263.

Sues, H.-D., J. A. Hopson, & N. H. Shubin. (1992). Affinities of ? *Scalenodontoides plemmyridon* Hopson, 1984 (Synapsida: Cynodontia) from the Upper Triassic of Nova Scotia. *Journal of Vertebrate Paleontology*, *12*, 168–171.

Sues, H. D., & Olsen, P. (2015). Stratigraphic and temporal context and faunal diversity of Permian-Jurassic continental tetrapod assemblages from the Fundy rift basin, eastern Canada. *Atlantic Geology*, *51*, 139–205.

Sues, H.-D., P. E. Olsen, T. J. Fedak, & R. R. Schoch. (2022). Diverse assemblage of Middle Triassic continental tetrapods from the Newark Supergroup of Nova Scotia (Canada). *Journal of Vertebrate Paleontology 41*, e2023168.

Sulej, T., & G. Niedźwiedzki. (2019). An elephant-sized Late Triassic synapsid with erect limbs. *Science*, *363*, 78–80.

Sulej, T., Bronowicz, R., Tałanda, M. & Niedźwiedzki, G. (2011). A new dicynodont-archosaur assemblage from the Late Triassic (Carnian) of Poland. *Earth & Environmental Science Transactions of The Royal Society of Edinburgh*, *101*, 261–269.

Surkov, M. V., & M. J. Benton. (2004). The basicranium of dicynodonts (Synapsida) and its use in phylogenetic analysis. *Palaeontology*, *47*, 619–638.

Szczygielski, T., & T. Sulej. (2021). A new stahleckeriid from Poland. *Journal of Vertebrate Paleontology, Programs and Abstracts*, *20*.

Szczygielski, T., & T. Sulej. (2023). *Woznikella triradiata*—a new kannemeyeriiform dicynodont from the Late Triassic of northern Pangea and the global distribution of Triassic dicynodonts. *Comptes Rendus Paleovol*, *22*, 279–406.

Whitney, M. R., Angielczyk, K. D., Peecook, B. R., & Sidor, C. A. (2021). The evolution of the synapsid tusk: insights from dicynodont therapsid tusk histology. *Proceedings of the Royal Society B*, *288*(1961), 20211670.

Williston, S. W. (1904). Notice of some new reptiles from the Upper Trias of Wyoming. *Journal of Geology*, *12*, 688–697.

APPENDIX 1.

List of character states coded for *Argodicynodon* and added to the matrix of Szczygielski and Sulej (2023). Character states were partitioned into "continuous" and "numeric" subsets and analyzed in TNT 1.5 using the method of Goloboff et al. (2006).

Continuous states (Szczygielski & Sulej, 2023: characters 1 through 23).
Argodicynodon
? ? ? ? ? ? ? ? ? ? ? ? ? 0.206 0.95 0.912 0.302 ? ? 0.86 2.3 ? 0.33

Discrete (numeric) states. Characters 1 through 176 below are based on Szczygielski and Sulej (2023) characters 24 through 199.
Argodicynodon
????????????0020???0?22??11?0000?????0111012011
(02)01110102201012011?0????????????????????????
0221220?????0010?1112???2001301211011101111121??
011100110010????0????????????1??1?